

A Free Lunch from the Noise: Provable and Practical Exploration for Representation Learning

Tongzheng Ren^{1, 2, *}Tianjun Zhang^{3, *}Csaba Szepesvári^{4, 5}Bo Dai²¹Department of Computer Science, UT Austin²Google Research, Brain Team³Department of EECS, UC Berkeley⁴DeepMind⁵Department of Computer Science, University of Alberta

Abstract

Representation learning lies at the heart of the empirical success of deep learning for dealing with the curse of dimensionality. However, the power of representation learning has not been fully exploited yet in reinforcement learning (RL), due to **i**), the trade-off between expressiveness and tractability; and **ii**), the coupling between exploration and representation learning. In this paper, we first reveal the fact that under some noise assumption in the stochastic control model, we can obtain the linear spectral feature of its corresponding Markov transition operator in closed-form *for free*. Based on this observation, we propose *Spectral Dynamics Embedding (SPEDE)*, which breaks the trade-off and completes optimistic exploration for representation learning by exploiting the structure of the noise. We provide rigorous theoretical analysis of SPEDE, and demonstrate the practical superior performance over the existing state-of-the-art empirical algorithms on several benchmarks.

1 INTRODUCTION

Reinforcement learning (RL) dedicates to solve the sequential decision making problem, where an agent is interacting with an *unknown* environment to find the best policy that maximizes the expected cumulative rewards [Sutton and Barto, 2018]. It is known that the tabular algorithms direct controlling over the original state and action in Markov decision processes (MDPs) achieve the minimax-optimal regret depending on the cardinality of the state and action space [Jaksch et al., 2010, Azar et al., 2017, Jin et al., 2018]. However, these algorithms become computationally intractable for the real-world problems with an enormous number of states. Learning with function approximations

upon *good* representation is a natural idea to tackle such computational issue, which has already demonstrated its effectiveness in the success of deep learning [Bengio et al., 2013]. In fact, representation learning lies at the heart of the empirical successes of deep RL in video games [Mnih et al., 2013], robotics [Levine et al., 2016], Go [Silver et al., 2017] to name a few. Meanwhile, the importance and benefits of the representation in RL is rigorously justified [Jin et al., 2020, Yang and Wang, 2020], which quantifies the regret in terms of the dimension of the *known* representation based on a subclass in MDPs [Puterman, 2014]. A natural question raises:

How to design provably efficient and practical algorithm for representation learning in RL?

Here, by “provably efficient” we mean the sample complexity of the algorithm can be rigorously characterized only in terms of the complexity of representation class, without explicit dependency on the number of states and actions, while by “practical” we mean the algorithm can be implemented and deployed for the real-world applications. Therefore, we not only require the representation learned is expressive enough for handling complex practical environments, but also require the operations in the algorithm tractable and computation/memory efficient. The major difficulty of this question lies in two-fold:

- i)** The *trade-off* between the expressiveness and the tractability in the design of the representations;
- ii)** The learning of representation is intimately *coupled* with exploration.

Specifically, a desired representation should be sufficiently expressive to capture the practical dynamic systems, while still computationally tractable. However, in general, expressive representation leads to complicated optimization in

* Equal Contribution

For a formal definition of expressiveness, see [Agarwal et al., 2020a].

learning. For example, the representation in the linear MDP is *exponentially stronger* than the latent variable MDPs in terms of expressiveness [Agarwal et al., 2020a]. However, its representation learning depends on either a MLE oracle that is computationally intractable due to the constraint on the regularity of conditional density [Agarwal et al., 2020a], or an optimization oracle that can solve complicated constrained min-max-min-max optimization [Modi et al., 2021]. On the other hand, Misra et al. [2020] considers the representation introduced by an encoder in block MDP [Du et al., 2019], in which the learning problem can be completed by a regression, but with the payoff that the representations in block MDP is even weaker than the latent variable MDP [Agarwal et al., 2020a].

Meanwhile, the coupling of the representation learning and exploration also induces the difficulty in *practical* algorithm design and analysis. Specifically, one cannot learn a precise representation without enough experiences from a comprehensive exploration, while the exploration depends on a reliable estimation of the representation. Most of the known results depends on a policy-cover-based exploration [Du et al., 2019, Misra et al., 2020, Agarwal et al., 2020a, Modi et al., 2021], which maintains and samples a set of policies during training for systematic exploration, that significantly increases the computation and memory cost in implementation.

In this work, we propose *Spectral Dynamics Embedding (SPEDE)*, dealing with the aforementioned difficulties appropriately, and thus, answering the question affirmatively. SPEDE is established on a connection between the stochastic control dynamics [Osband and Van Roy, 2014, Kakade et al., 2020] and linear MDPs in Section 3. Specifically, by exploiting the property of the *noise* in the stochastic control dynamics, we can recover the factorization of its corresponding Markov transition operator in closed-form *without extra computation*. This equivalency immediately overcomes the computational intractability in the linear MDP estimation via the corresponding control dynamics form, and thus, breaks the trade-off between expressiveness and tractability. Meanwhile, as a byproduct, the linear MDP reformulation also introduce efficient planning for optimal policy in nonlinear control through the linear sufficient feature from the spectral space of Markov operator, while in most model-based RL, planning is conducted by treating learned model as simulator, and thus, is inefficient and suboptimal.

More importantly, the two faces of one model also provide the opportunity to tackle the coupling between representation learning and exploration. The optimism in the face of uncertainty principle can be easily implemented through Thompson sampling w.r.t. the stochastic nonlinear dynamics, which leads to the posterior of representations implicitly, while bypasses the unidentifiability issue in directly characterizing the representation, therefore, can be theoretically

justified.

We rigorously characterize the statistical property of SPEDE in terms of regret w.r.t. the complexity of representation class in Section 4, without explicit dependence on the size of raw state space and action space. With the established unified view, our results generalize online control [Kakade et al., 2020] and linear MDP [Jin et al., 2020] beyond *known* features. We finally demonstrate the superiority of SPEDE on the MuJoCo benchmarks in Section 5. It significantly outperforms the empirical state-of-the-art RL algorithms. To our knowledge, SPEDE is the first representation learning algorithm achieving statistical, computational, and memory efficiency with sufficient expressiveness.

1.1 RELATED WORK

There have been many great attempts on **algorithmic representation learning** in RL for different purposes, *e.g.*, bisimulation [Ferns et al., 2004, Gelada et al., 2019], reconstruction [Hafner et al., 2019]. Recently, there are also several works considering the spectral features based on decomposing different variants of the transition operator, including successor features [Dayan, 1993, Kulkarni et al., 2016], proto-value functions [Mahadevan and Maggioni, 2007, Wu et al., 2018], spectral state-aggregation [Duan et al., 2018, Zhang and Wang, 2019], and contrastive fourier features [Nachum and Yang, 2021]. These works are highly-related to the proposed SPEDE. Besides these features focus on *state-only* representation, the major differences between SPEDE and these spectral features lie in **i)**, the target operators in existing spectral features are *state-state* transition, which cancel the effect of action; **ii)**, the target operators are estimated based on empirical data from a *fixed behavior policy* under the implicit assumption that the estimated operator is *uniformly accurate*, ignoring the major difficulty in exploration, while SPEDE carefully designed the systematic exploration with theoretical guarantee; **iii)**, most of the existing spectral features rely on *explicitly* decomposition of the operators, while SPEDE obtains the spectral *for free*.

Turning to the **theoretically-justified representation learning with online exploration**, a large body of effort focuses on the policy-cover-based exploration [Du et al., 2019, Misra et al., 2020, Agarwal et al., 2020a, Modi et al., 2021]. The major difficulty impedes their practical application is the computation and memory cost: the policy-cover-based exploration requires a set of exploratory policies to be maintained and sampled from during training, which can be extremely expensive. Uehara et al. [2021] introduced a UCB mechanism that can enforce exploration without the requirements on maintaining the policy cover. However, the algorithm requires an MLE oracle for unnormalized conditional statistical model, which still prevents us from applying the algorithm in practice until recent attempt [Zhang

et al., 2022] using contrastive learning to replace the MLE.

Another two related lines of research are **model-based RL** and **online control**, which are commonly known overlapped but separate communities considering different formulations of the dynamics. Our finding bridges these two communities by establishing the equivalency between standard models that are widely considered in the corresponding communities. Osband and Van Roy [2014] and Kakade et al. [2020] are the most related to our work in each community. These models generalize their corresponded linear models, *i.e.*, Jin et al. [2020] and Cohen et al. [2019], with general nonlinear model and kernel function within a known RKHS, respectively. The regret of the optimistic (pessimistic) algorithm has been carefully characterized for these models. However, both of the proposed algorithms in Osband and Van Roy [2014] and Kakade et al. [2020] require a planning oracle to seek the optimal policy, which might be computationally intractable. In SPEDE, this is easily handled in the equivalent linear MDP.

2 PRELIMINARIES

Markov Decision Process (MDP) is one of the most standard models studied in the reinforcement learning that can be denoted by the tuple $\mathcal{M} = (\mathcal{S}, \mathcal{A}, r, T, \rho, H)$, where \mathcal{S} is the state space, \mathcal{A} is the action space, $r : \mathcal{S} \times \mathcal{A} \rightarrow \mathbb{R}^+$ is the reward function (where \mathbb{R}^+ denotes the set of non-negative real numbers), $T : \mathcal{S} \times \mathcal{A} \rightarrow \Delta(\mathcal{S})$ is the transition and ρ is an initial state distribution and H is the horizon (*i.e.*, the length of each episode). A (potentially non-stationary) policy π can be defined as $\{\pi_h\}_{h \in [H]}$ where $\pi_h : \mathcal{S} \rightarrow \Delta(\mathcal{A}), \forall h \in [H]$. Following the standard notation, we define the value function $V_h^\pi(s_h) := \mathbb{E}_{T, \pi} \left[\sum_{t=h}^{H-1} r(s_t, a_t) | s_h = s \right]$ and the action-value function (*i.e.*, the Q function) $Q_h^\pi(s_h, a_h) = \mathbb{E}_{T, \pi} \left[\sum_{t=h}^{H-1} r(s_t, a_t) | s_h = s, a_h = a \right]$, which are the expected cumulative rewards under transition T when executing policy π starting from s_h and (s_h, a_h) . With these two definitions at hand, it is straightforward to show the following Bellman equation:

$$Q_h^\pi(s_h, a_h) = r(s_h, a_h) + \mathbb{E}_{s_{h+1} \sim T(\cdot | s_h, a_h)} [V_{h+1}^\pi(s_{h+1})].$$

Most of RL algorithms aim at finding the optimal policy $\pi^* = \arg \max_{\pi} \mathbb{E}_{s \sim \rho} [V_0^\pi(s)]$ under MDPs. It is well known that in the tabular setting when the state space and action space are finite, we can provably identify the optimal policy with both sample-efficient and computational-efficient optimism-based methods [*e.g.* Azar et al., 2017]

In general, the reward can be stochastic. Here for simplicity we assume the reward is deterministic and known throughout the paper, which is a common assumption in the literature [*e.g.*, Jin et al., 2018, 2020, Kakade et al., 2020].

Our method can be generalized to infinite horizon case, see Section 3.2 for the detail.

with the complexity proportion to $\text{poly}(|\mathcal{S}|, |\mathcal{A}|)$. However, in practice, the cardinality of state and action space can be large or even infinite. Hence, we need to incorporate function approximation into the learning algorithm when we deal with such cases. The linear MDP [Yang and Wang, 2019, Jin et al., 2020, Yang and Wang, 2020] or low-rank MDP [Agarwal et al., 2020a, Modi et al., 2021] is the most well-known MDP class that can incorporate linear function approximation with theoretical guarantee, thanks to the following assumption on the transition and reward:

$$T(s' | s, a) = \langle \phi(s, a), \mu(s') \rangle_{\mathcal{H}}, \quad r(s, a) = \langle \phi(s, a), \theta \rangle_{\mathcal{H}}, \quad (1)$$

where $\phi : \mathcal{S} \times \mathcal{A} \rightarrow \mathcal{H}, \mu : \mathcal{S} \rightarrow \mathcal{H}$ are two feature maps and \mathcal{H} is a Hilbert space. The most essential observation for them is that, $Q_h^\pi(s, a)$ for any policy π is linear w.r.t $\phi(s_h, a_h)$, due to the following observation [Jin et al., 2020]:

$$\begin{aligned} Q_h^\pi(s_h, a_h) &= r(s_h, a_h) + \int V_{h+1}^\pi(s_{h+1}) T(s_{h+1} | s_h, a_h) ds_{h+1} \\ &= \left\langle \phi(s_h, a_h), \theta + \int V_{h+1}^\pi(s_{h+1}) \mu(s_{h+1}) ds_{h+1} \right\rangle_{\mathcal{H}}. \end{aligned} \quad (2)$$

Therefore, ϕ serves as a sufficient representation for the estimation of Q_h^π , that can provide uncertainty estimation with standard linear model analysis and eventually lead to sample-efficient learning when ϕ is fixed and known to the agent [see Theorem 3.1 in Jin et al., 2020]. However, we in general do not have such representations in advance and we need to learn the representation from the data, which constraints the applicability of the algorithms derived with fixed and known representation.

Remark (Model-based RL vs. RL with Representation):

We would like to emphasize that, although most of the existing representation learning methods need to learn the transition [Du et al., 2019, Misra et al., 2020, Agarwal et al., 2020a, Uehara et al., 2021], RL with representation learning is related but perpendicular to the concept of model-based RL. The major difference lies in how to use the learned transition for planning (*i.e.* finding the optimal policy). In vanilla model-based RL methods [*e.g.*, Sutton, 1990, Chua et al., 2018, Kurutach et al., 2018], the learned transition is played as a simulator generating samples for policy improvement; while in representation-based RL, the representation is extracted from the learned transition to compose the policy explicitly, which is significantly efficient comparing to the model-based RL methods.

One exception is the tabular MDP, where we can choose $\phi : \mathcal{S} \times \mathcal{A} \rightarrow \mathbb{R}^{|\mathcal{S}| \cdot |\mathcal{A}|}$ that each state-action pair has exclusive one non-zero element and $\mu : \mathcal{S} \rightarrow \mathbb{R}^{|\mathcal{S}| \cdot |\mathcal{A}|}$ correspondingly defined to make (1) hold.

3 SPECTRAL DYNAMICS EMBEDDING

It is naturally to consider how to perform sample-efficient representation learning (and hence sample-efficient reinforcement learning) that satisfies (1) in an online manner. The most straightforward idea is performing the maximum likelihood estimation (MLE) in the representation space [e.g., Agarwal et al., 2020a]. Unfortunately, for general cases, such MLE is intractable, due to the constraints on the regularity of marginal distribution (i.e., $\langle \phi(s, a), \int_{s'} \mu(s') ds' \rangle = 1$) for all $(s, a) \in \mathcal{S} \times \mathcal{A}$. Moreover, even we can perform MLE for certain cases (for example, the block MDP), as the representation is estimated from the data, which can be inaccurate, most of the existing work apply the policy cover technique [Du et al., 2019, Misra et al., 2020, Agarwal et al., 2020a, Modi et al., 2021] to enforce exploration. However, such procedures can be both computational and memory expensive when we need amounts of exploratory policy to guarantee the coverage of whole state space, which makes it not a practical choice.

To overcome these issues, we introduce Spectral Dynamics Embedding (SPEDE), which leverages the noise structure to provide a simple but provable efficient and practical algorithm for representation learning in RL. We first introduce our key observation, which induces the equivalency between linear MDP and stochastic nonlinear control.

3.1 KEY OBSERVATION

Our fundamental observation is that, the density of isotropic Gaussian distribution can be expressed as the inner product of two feature maps, thanks to the reproducing property and the random Fourier transform of the Gaussian kernel [Rahimi and Recht, 2007]:

$$\begin{aligned} \phi(x|\mu, \sigma^2 I) &\propto \exp\left(-\frac{\|x - \mu\|^2}{2\sigma^2}\right) \\ &= \langle k(x, \cdot), k(\mu, \cdot) \rangle_{\mathcal{H}} \quad (\text{Reproducing Property}) \end{aligned} \quad (3)$$

$$= \langle \varphi(x, \omega, b), \varphi(\mu, \omega, b) \rangle_{p(\omega, b)} \quad (\text{Random Fourier}), \quad (4)$$

where $k(\cdot, \cdot)$ is the Gaussian kernel with bandwidth σ : $k(x, y) = \exp\left(-\frac{\|x - y\|_2^2}{2\sigma^2}\right)$, \mathcal{H} is the Reproducing Kernel Hilbert Space (RKHS) associated with k , $\varphi(x, \omega, b) = \sqrt{2} \cos(\omega^\top x + b)$, $\langle f, g \rangle_p = \mathbb{E}_{p(x)}[f(x)g(x)]$ and $p(\omega, b) = \mathcal{N}(\omega; 0, 1/\sigma^2 I) \cdot \mathcal{U}(b; [0, 2\pi])$ with \mathcal{N} and \mathcal{U} denoting Gaussian and Uniform distribution, respectively.

¹We provide a brief review on the related definitions in Appendix A.

Consider the general transition dynamics,

$$s' = f^*(s, a) + \epsilon, \quad \epsilon \sim \mathcal{N}(0, \sigma^2), \quad (5)$$

$$\text{or equivalently } T(s'|s, a) \propto \exp\left(-\frac{\|s' - f^*(s, a)\|^2}{2\sigma^2}\right), \quad (6)$$

which is a widely used setup in the empirical model-based reinforcement learning [e.g., Chua et al., 2018, Kurutach et al., 2018, Clavera et al., 2018, Wang et al., 2019], and the online (non)-linear control [e.g., Abbasi-Yadkori and Szepesvári, 2011, Mania et al., 2019, 2020, Simchowitz and Foster, 2020, Kakade et al., 2020]. Here $s \in \mathbb{R}^d$, $a \in \mathcal{A}$ that can be continuous and f^* is a dynamic function.

By applying the reproducing property (3) or random Fourier transform (4) for the transition dynamics (5), we can obtain the feature ϕ and μ satisfies (1) *for free*. Specifically, taking the reproducing property as an example, we have that

$$T(s'|s, a) = \langle k(f^*(s, a), \cdot), (2\pi\sigma^2)^{-d/2} k(s', \cdot) \rangle_{\mathcal{H}}, \quad (7)$$

which means the problem (5) is indeed a linear MDP with $\phi(s, a) = k(f^*(s, a), \cdot)$ and $\mu(s') = (2\pi\sigma^2)^{-d/2} k(s', \cdot)$. Following (2), we know $Q(s, a)$ is in the linear span of the $\phi(s, a)$ that is transformed from $f^*(s, a)$. Therefore, finding a good representation of $Q(s, a)$ is equivalent to finding a good estimation of f^* . In the next section, we will show that, with the well-known optimism in the face of uncertainty (OFU) principle, we can estimate f^* in an online manner with a both sample-efficient in terms of regret and computational-efficient algorithm.

Remark (Computation-free Factorizable Noise Model):

We remark that, similar observations also hold for large amounts of distributions, e.g., the Laplace and Cauchy distribution. We refer the interested reader to Table 1 in Dai et al. [2014] for the known transformation of kernels and features. Here we focus on the Gaussian noise.

Remark (Reward Factorization):

In the definition of linear MDP (1), the reward function $r(s, a)$ should also have the ability to be linearly represented by $\phi(s, a)$. This can be implemented by augmenting $[\phi(s, a), r(s, a)]$ as the new representation, therefore, we neglect the reward function throughout the paper.

3.2 PRACTICAL ALGORITHM DESCRIPTION

Here, we introduce a generic Thompson Sampling (TS) type algorithm in Algorithm 1 based on the OFU principle that leverage our observation at the previous section. At the beginning, we provide a prior distribution $\mathbb{P}(f)$ that reflects our prior knowledge on f^* . Then for each episode, we draw a f from the posterior, find the optimal policy with f using the planning algorithm, execute this policy and eventually

Algorithm 1 Thompson Sampling (TS) Algorithm

Require: Number of Episodes K , Prior Distribution $\mathbb{P}(f)$,
Reward Function $r(s, a)$.

- 1: Initialize the history set $\mathcal{H}_0 = \emptyset$.
- 2: **for** episodes $k = 1, 2, \dots$ **do**
- 3: **Sample** $f_k \sim \mathbb{P}(f|\mathcal{H}_k)$. \triangleright Draw the Representation.
- 4: **Find the optimal policy** π_k on f_k with Algorithm 2.
 \triangleright Planning with f_k .
- 5: **for** steps $h = 0, 1, \dots, H - 1$ **do** \triangleright Executing π_k .
- 6: Execute $a_h^k \sim \pi_k^h(s_h^k)$.
- 7: Observe s_{h+1} .
- 8: **end for**
- 9: Set $\mathcal{H}_k = \mathcal{H}_{k-1} \cup \{(s_h^k, a_h^k, s_{h+1}^k)\}_{h=0}^{H-1}$. \triangleright Update the History.
- 10: **end for**

inference the posterior with the new observation. Notice that, we choose the policy optimistically with an *sampled* f , which enforces the exploration following the principle of OFU. Meanwhile, we only learn the dynamic with posterior inference and directly obtain the representation with (3) or (4), which avoids additional error from the representation learning step. As all of our data is collected with f^* , our posterior will shrink to a point mass of f^* , which guarantees we can identify good representation and good policy with sufficient number of data.

One significant part of SPEDE is the computational-efficient planning with f_k , thanks to the linear MDP formulation (7). Prior work assumes an oracle [e.g., Kakade et al., 2020] for such planning problem, but little is known on how to provably perform such planning efficiently. Notice that, with the feature $\phi(s, a)$ defined via (3) and (4), we know that $Q_h^\pi(s, a)$ is exactly linear in $\phi(s, a)$, $\forall h, \pi$. Hence, we can perform a dynamic programming style algorithm that calculates $Q_h^\pi(s, a)$ with the given feature $\phi(s, a)$, and then greedily select the action at each level h , which is simple yet efficient. It is straightforward to show that the policy obtained with this dynamic programming algorithm is optimal by induction. We illustrate the detailed algorithm in Algorithm 2.

3.2.1 Implementation Details

In such a planning algorithm, we need to maintain the posterior of f and calculate the term $\int V_{h+1}(s')\mu(s') ds'$ and take the maximum of $Q_h(s, a)$ over a , which can be problematic. We will provide more discussion on this issue below.

Posterior Sampling The exact posterior inference can be hard if f^* does not lie in simple function class (e.g., linear function class) or has some derived property (e.g., conjugacy), so in practice we apply the existing mature

Algorithm 2 Planning with Dynamic Programming

Require: Transition Model f , Reward Function $r(s, a)$.

- 1: Initialize $\phi(s, a), \mu(s')$ with (3) or (4). $V_H(s) = 0, \forall s$.
- 2: **for** steps $h = H - 1, H - 2, \dots, 0$ **do**
- 3: **Compute**
$$Q_h(s, a) = r(s, a) + \langle \phi(s, a), \int V_{h+1}(s')\mu(s') ds' \rangle_{\mathcal{H}}.$$

 \triangleright Bellman Update.
- 4: Set $V_h(s) = \max_a Q_h(s, a), \pi_h(s) = \arg \max_a Q_h(s, a)$. \triangleright Choose the Optimal Policy.
- 5: **end for**
- 6: **return** $\{\pi_h\}_{h=0}^{H-1}$.

approximate inference methods like Markov Chain Monte Carlo (MCMC) [e.g., Neal et al., 2011] and variational inference [see, Blei et al., 2017]. In our implementation, we used stochastic gradient langevin dynamics [Welling and Teh, 2011, Cheng and Bartlett, 2018] to train an ensemble of models for posterior approximation.

Large State and Action Space In general, we need to handle the case when the number of states and actions can be large, or even infinite. Notice that, when the state space is large, we can estimate the term $\int V_{h+1}(s')\mu(s') ds'$ with regression based method using the samples from f [Antos et al., 2008]. For the continuous action space, we can apply principled policy optimization methods [e.g., Agarwal et al., 2020b] with an energy-based model (EBM) parametrized policy [Nachum et al., 2017, Dai et al., 2018], treat the linear $Q^\pi(s, a)$ as the gradient and perform mirror descent and eventually obtain the optimal policy. However, this is at the cost of an additional sampling step from the EBM policy. In practice, we introduce a Gaussian policy and perform soft actor-critic [Haarnoja et al., 2018] policy update, which already provides good empirical performance. To sum up, for large state and action cases, we learn the critic in the learned representation space by regression, and obtain the Gaussian parametrized actor with SAC policy update step, in Line 3 and 4 in Algorithm 2, respectively.

Infinite Horizon Case Our algorithm can be provably extended to the infinite horizon case with specific termination condition for each episode [e.g., see Jaksch et al., 2010]. In practice, for the planning part we can solve the linear fixed-point equation with the feature $\phi(s, a)$ using the popular algorithms like Fitted Q -iteration (FQI) [Antos et al., 2008] or dual embedding [Dai et al., 2018]. that still guarantees to find the optimal policy.

4 THEORETICAL GUARANTEES

In this section, we provide theoretical justification for SPEDE, showing that SPEDE can identify informative representation and as a result, near-optimal policy in a sample-efficient way.

We first define the notation of regret. Assume at episode k , the learner chooses the policy π_k and observes a sequence $\{(s_h^k, a_h^k)\}_{h=0}^{H-1}$. We define the regret of the first K episodes (and define $T := KH$) as:

$$\text{Regret}(K) := \sum_{k \in [K]} [V_0^*(s_0^k) - V_0^{\pi_k}(s_0^k)] \quad (8)$$

The regret measures the sample complexity of the representation learning in RL. We want to provide a regret upper bound that is sublinear in T . When T increases, we collect more data that can help us build a much more accurate estimation on the representation, which should decrease the per-step regret and make the overall regret scale sublinear in T . As we consider the Thompson Sampling algorithm, we would like to study the expected regret $\mathbb{E}_{\mathbb{P}(f)}[\text{Regret}(K)]$, which takes the prior $\mathbb{P}(f)$ into account.

4.1 ASSUMPTIONS

Before we start, we first state the assumptions we use to derive our theoretical results.

We assume the reward is bounded, which is common in the literature [e.g. Azar et al., 2017, Jin et al., 2018, 2020].

Assumption 1 (Bounded Reward). $r(s, a) \in [0, 1]$, $\forall (s, a) \in \mathcal{S} \times \mathcal{A}$.

In practice, we generally approximate f^* with some complicated function approximators, so we focus on the setting where we want to find f^* from a general function class \mathcal{F} . This is important for MuJoCo dynamics modeling, which have complicated transitions over angle, angular velocity and torque of the agent in the raw state. We first state some necessary definitions and assumptions on \mathcal{F} .

Definition 1 (ℓ_2 -norm of functions). Define $\|f\|_2 := \max_{(s,a) \in \mathcal{S} \times \mathcal{A}} \|f(s, a)\|_2$. Notice that it is not the commonly used ℓ_2 norm for the function, but it suits our purpose well.

Assumption 2 (Bounded Output). We assume that $\|f\|_2 \leq C$, $\forall f \in \mathcal{F}$.

Assumption 3 (Realizability). We assume the ground truth dynamic function $f^* \in \mathcal{F}$.

We then define the notion of covering number, which will be helpful in our algorithm derivation.

Definition 2 (Covering Number [Wainwright, 2019]). An ϵ -cover of \mathcal{F} with respect to a metric ρ is a set $\{f_i\}_{i \in [n]} \subseteq \mathcal{F}$, such that $\forall f \in \mathcal{F}$, there exists $i \in [n]$, $\rho(f, f_i) \leq \epsilon$. The ϵ -covering number is the cardinality of the smallest ϵ -cover, denoted as $\mathcal{N}(\mathcal{F}, \epsilon, \rho)$.

Assumption 4 (Bounded Covering Number). We assume that $\mathcal{N}(\mathcal{F}, \epsilon, \|\cdot\|_2) < \infty$, $\forall \epsilon > 0$.

Remark Basically, Assumption 2 means the the transition dynamic never pushes the state far from the origin, which holds widely in practice. Assumption 3 guarantees that we can find the exact f^* in \mathcal{F} , or we will always suffer from the error induced by model mismatch. Assumption 4 ensures that we can estimate f^* with small error when we have sufficient number of observations.

Besides the bounded covering number, we also need an additional assumption on bounded eluder dimension, which is defined in the following:

Definition 3 (ϵ -dependency [Osband and Van Roy, 2014]). A state-action pair $(s, a) \in \mathcal{S} \times \mathcal{A}$ is ϵ -dependent on $\{(s_i, a_i)\}_{i \in [n]} \subseteq \mathcal{S} \times \mathcal{A}$ with respect to \mathcal{F} , if $\forall f, \tilde{f} \in \mathcal{F}$ satisfying $\sqrt{\sum_{i \in [n]} \|f(s_i, a_i) - \tilde{f}(s_i, a_i)\|_2^2} \leq \epsilon$ satisfies that $\|f(s, a) - \tilde{f}(s, a)\|_2 \leq \epsilon$. Furthermore, (s, a) is said to be ϵ -independent of $\{(s_i, a_i)\}_{i \in [n]}$ with respect to \mathcal{F} if it is not ϵ -dependent on $\{(s_i, a_i)\}_{i \in [n]}$.

Definition 4 (Eluder Dimension [Osband and Van Roy, 2014]). We define the eluder dimension $\text{dim}_E(\mathcal{F}, \epsilon)$ as the length d of the longest sequence of elements in $\mathcal{S} \times \mathcal{A}$, such that $\exists \epsilon' \geq \epsilon$, every element is ϵ' -independent of its predecessors.

Remark Intuitively, eluder dimension illustrates the number of samples we need to make our prediction on unseen data accurate. If the eluder dimension is unbounded, then we cannot make any meaningful prediction on unseen data even with large amounts of collected samples. Hence, to make the learning possible, we need the following bounded eluder dimension assumption.

Assumption 5 (Bounded Eluder Dimension). We assume $\text{dim}_E(\mathcal{F}, \epsilon) < \infty$, $\forall \epsilon > 0$.

4.2 MAIN RESULT

Theorem 5 (Regret Bound). Assume Assumption 2 to 5 holds. We have that

$$\mathbb{E}_{\mathbb{P}(f)}[\text{Regret}(K)] \leq \tilde{O}\left(\sqrt{H^2 T} \cdot \sqrt{\log \mathcal{N}(\mathcal{F}, T^{-1/2}, \|\cdot\|_2)} \cdot \sqrt{\text{dim}_E(\mathcal{F}, T^{-1/2})}\right).$$

where \tilde{O} represents the order up to logarithm factors.

For finite dimensional function class, $\log \mathcal{N}(\mathcal{F}, T^{-1/2}, \|\cdot\|_2)$ and $\dim_E(\mathcal{F}, T^{-1/2})$ should be scaled like $\text{polylog}(T)$, hence our upper bound is sublinear in T . The proof is in Appendix C. Here we briefly sketch the proof idea.

Proof Sketch. We first construct an equivalent UCB algorithm (see Appendix B) and bound $\text{Regret}(K)$ for it. Then by the conclusion from Russo and Van Roy [2013, 2014], Osband and Van Roy [2014], we can directly translate the upper bound on $\text{Regret}(K)$ from UCB algorithm to an upper bound on $\mathbb{E}_{\mathbb{P}(f)}[\text{Regret}(K)]$ of TS algorithm. We emphasize that the UCB algorithm is solely designed for analysis purpose.

With the optimism, we know for episode k , $V_0^*(s_0^k) \leq \tilde{V}_{0,k}^{\pi_k}(s_0^k)$, where $\tilde{V}_{h,k}^{\pi_k}$ is the value function of policy π_k under the model \tilde{f}_k introduced in the UCB algorithm. Hence, the regret at episode k can be bounded by $\tilde{V}_{0,k}^{\pi_k}(s_0^k) - V_0^{\pi_k}(s_0^k)$, which is the value difference of the policy π_k under the two models \tilde{f}_k and f^* , that can be bounded by $\sqrt{\mathbb{E} \left[\sum_{h=0}^{H-1} \|f^*(s_h^k, a_h^k) - \tilde{f}_k(s_h^k, a_h^k)\|_2^2 \right]}$ (see Lemma 14 for the details), which means when the estimated model \hat{f} is close to the real model f^* , the policy obtained by planning on \hat{f} will only suffer from a small regret. With Cauchy-Schwartz inequality, we only need to bound $\mathbb{E} \left[\sum_{k \in [K]} \sum_{h=0}^{H-1} \|f^*(s_h^k, a_h^k) - \tilde{f}_k(s_h^k, a_h^k)\|_2^2 \right]$. This term can be handled via Lemma 18. With some additional technical steps, we can obtain the upper bound on $\text{Regret}(K)$ for the UCB algorithm, and hence the upper bound on $\mathbb{E}_{\mathbb{P}(f)}[\text{Regret}(K)]$ for the TS algorithm. \square

Kernelized Non-linear Regulator Notice that, for the linear function class $\mathcal{F} = \{\theta^\top \varphi(s, a) : \theta \in \mathbb{R}^{d_\varphi \times d}\}$ where $\varphi : \mathcal{S} \times \mathcal{A} \rightarrow \mathbb{R}^{d_\varphi}$ is a fixed and known feature map of certain RKHS, when the feature and the parameters are bounded, the logarithm covering number can be bounded by $\log \mathcal{N}(\mathcal{F}, \epsilon, \|\cdot\|_2) \lesssim d_\varphi \log(1/\epsilon)$, and the eluder dimension can be bounded by $\dim_E(\mathcal{F}, \epsilon) \lesssim d_\varphi \log(1/\epsilon)$ (see Appendix D for the detail, notice that we provide a tighter bound of the eluder dimension compared with the one derived in Osband and Van Roy [2014]). Hence, for linear function class, Theorem 5 can be translated into a regret upper bound of $\tilde{O}(H d_\varphi T^{1/2})$ for sufficiently large T , that matches the results of Kakade et al. [2020]. Moreover, for the case of linear bandits when $H = 1$, our bound can be

Note that, the RKHS here is the Hilbert space that contains $f(s, a)$ with the feature from some fixed and known kernel, It is different from the RKHS we introduced in Section 3, that contains $Q(s, a)$ with the feature $k(f(s, a), \cdot)$ where k is the Gaussian kernel.

Note that T in [Kakade et al., 2020] is the number of episodes, and V_{\max} in [Kakade et al., 2020] can be viewed as H^2 when the per-step reward is bounded.

translated into a regret upper bound of $\tilde{O}(d_\varphi T^{1/2})$, that matches the lower bound [Dani et al., 2008] up to logarithmic terms.

Compared with Kakade et al. [2020] and Osband and Van Roy [2014] Our results have some connections with the results from Kakade et al. [2020] and Osband and Van Roy [2014]. However, in Kakade et al. [2020], the authors only considers the case when \mathcal{F} only contains linear functions w.r.t some known feature map, which constrains its application in practice. We instead, consider the general function approximation, which makes our algorithm applicable for more complicated models like deep neural networks. Meanwhile, the regret bound from Osband and Van Roy [2014] depends on a global Lipschitz constant for the value function, which can be hard to quantify with either theoretical or empirical method. Instead, our regret bound gets rid of such dependency on the Lipschitz constant with the simulation lemma that carefully exploit the noise structure.

5 EXPERIMENTS

In this section, we study the empirical performance of SPEDE in the OpenAI MuJoCo control suite [Brockman et al., 2016]. We use the environments from MBBL [Wang et al., 2019], which varies slightly from the original environments in terms of modifying the reward function so its gradient w.r.t the states exists and introducing early termination (ET). Note that the set of environments contains various control and manipulation tasks, which are commonly used for benchmarking both model-free and model-based RL algorithms [e.g., Kakade et al., 2020, Haarnoja et al., 2018]. As aforementioned, for practical implementation, our critic network consists of a representation network $\phi(\cdot)$ and a linear layer on the top. We follow the same procedure of Algorithm 1. Specifically, (1) for finding the optimal policy, we run an actor-critic algorithm (SAC); (2) we fix the representation network of the critic function $\phi(\cdot)$ and only update the linear layer on the top. We provide the full set of experiments in Appendix E.2 and the hyperparameter we use in Appendix E.6.

Baselines We compare our method with various model-based RL baselines: PETS [Chua et al., 2018] with random shooting (RS) optimizer, PETS with cross entropy method (CEM) optimizer and ME with TRPO policy optimizer [Kurutach et al., 2018]. Note that these are strong empirical baselines with many hand-tuned hyperparameters and engineering features (e.g., ensemble of models). It is usually hard for any theoretically guaranteed model-based RL algorithm to match or surpass their performance [Kakade et al., 2020]. Another natural baseline is the successor feature [Dayan, 1993], which is one of the representative spectral features. We compare with the deep successor feature

Our code is available at <https://sites.google.com/view/spede>.

Table 1: Performance of SPEDE on various MuJoCo control tasks. All the results are averaged across 4 random seeds and a window size of 10K. Results marked with * is directly adopted from MBBL [Wang et al., 2019]. Our method achieves strong performance compared to pure empirical baselines (e.g., PETS). We also compare SPEDE-REG which regularizes the critic using the model dynamics loss with several model-free RL method. SPEDE-REG significantly improves the performance of the SoTA method SAC.

	Swimmer	Reacher	MountainCar	Pendulum	I-Pendulum
ME-TRPO*	30.1±9.7	-13.4±5.2	-42.5±26.6	177.3±1.9	-126.2±86.6
PETS-RS*	42.1±20.2	-40.1±6.9	-78.5±2.1	167.9±35.8	-12.1±25.1
PETS-CEM*	22.1±25.2	-12.3±5.2	-57.9±3.6	167.4±53.0	-20.5±28.9
DeepSF	25.5±13.5	-16.8±3.6	-17.0±23.4	168.6±5.1	-0.2±0.3
SPEDE	42.6±4.2	-7.2±1.1	50.3±1.1	169.5±0.6	0.0±0.0
PPO*	38.0±1.5	-17.2±0.9	27.1±13.1	163.4±8.0	-40.8±21.0
TRPO*	37.9±2.0	-10.1±0.6	-37.2±16.4	166.7±7.3	-27.6±15.8
TD3*	40.4±8.3	-14.0±0.9	-60.0±1.2	161.4±14.4	-224.5±0.4
SAC*	41.2±4.6	-6.4±0.5	52.6±0.6	168.2±9.5	-0.2±0.1
SPEDE-REG	40.0±3.8	-5.8±0.6	40.0±3.8	168.5±4.3	0.0±0.1
	Ant-ET	Hopper-ET	S-Humanoid-ET	Humanoid-ET	Walker-ET
ME-TRPO*	42.6±21.1	4.9±4.0	76.1±8.8	72.9±8.9	-9.5±4.6
PETS-RS*	130.0±148.1	205.8±36.5	320.9±182.2	106.9±106.9	-0.8±3.2
PETS-CEM*	81.6±145.8	129.3±36.0	355.1±157.1	110.8±91.0	-2.5±6.8
DeepSF	768.1±44.1	548.9±253.3	533.8±154.9	168.6±5.1	165.6±127.9
SPEDE	806.2±60.2	732.2±263.9	986.4±154.7	886.9±95.2	501.6±204.0
PPO*	80.1±17.3	758.0±62.0	454.3±36.7	451.4±39.1	306.1±17.2
TRPO*	116.8±47.3	237.4±33.5	281.3±10.9	289.8±5.2	229.5±27.1
TD3*	259.7±1.0	1057.1±29.5	1070.0±168.3	147.7±0.7	3299.7±1951.5
SAC*	2012.7±571.3	1815.5±655.1	834.6±313.1	1794.4±458.3	2216.4±678.7
SPEDE-REG	2073.1±119.7	2510.3±550.8	2710.3±277.5	3747.8±1078.1	2170.3±810.9

(DeepSF) [Kulkarni et al., 2016], and for a fair comparison, we only swap the representation objective of SPEDE with DeepSF and keep the other parts of the algorithm exactly the same.

SPEDE: Performance with the Learned Representation

Following Algorithm 1, we are interested in how SPEDE performs when we conduct planning on top of the representation induced by the dynamics model in each episode. As most of the rigorously-justified representation learning algorithms are computationally intractable/inefficient, to demonstrate the effectiveness of representation used in SPEDE, we compare SPEDE with the deep successor features, which is one representative empirical representation learning algorithm. Moreover, as our method learning representation via fitting transition dynamics, to demonstrate the superiority of representation in planning, we compare our methods with the state-of-the-art model-based RL algorithms. We summarize the results of our method in Table 1. We see that our method achieves impressive performance comparing to model-based RL methods. Even in some hard environments that baselines fail to reach positive reward (e.g., MountainCar, Walker-ET), SPEDE manage to achieve a reward of 52.6 and 501.6 respectively. We also evaluate our representation by comparing SPEDE to the usage of deep successor feature (DeepSF). Results show that on hard tasks like Humanoid and Walker, SPEDE manages to achieve 452.6 and 336.0 higher reward respectively.

SPEDE-REG: Policy Optimization with SPEDE Representation Regularizer In order to evaluate whether our assumption on linear MDP is valid in empirical settings

and study whether such assumption can help improve the performance, we add our model dynamics representation objective as a regularizer in addition to the original SAC algorithm for learning the Q -function. Specifically, the algorithm SPEDE-REG consists of vanilla SAC objective with an additional loss putting constraints on the representation learned by the critic function, due to the intuition that the representation should satisfy the equivalent dynamics. We compare its performance with the vanilla SAC algorithm to show the benefits of dynamic representation. Results in Table 1 show that adding such constraint significantly improve the performance of SAC: on hard tasks like Hopper-ET, S-Humanoid-ET and Humanoid-ET, SPEDE-REG improves the performance of SAC by 694.8, 1875.7 and 2000.4.

Ablations We conduct ablations on: (1) What is the effect of the momentum parameter. (2) How does the number of random features affect the performance. Detailed results can be found at E.3.

Performance Curves To better understand how the sample complexity of our algorithm comparing to the prior model-based RL baselines, we plot the return versus environment steps in Figure 1. We see that comparing to prior model-based baselines, SPEDE enjoys great sample efficiency in these tasks. We want to emphasize that from MBBL [Wang et al., 2019], model-based methods already show significantly better sample efficiency compared to model-free methods (e.g.PPO/TRPO). We provide additional results in Appendix E.2.

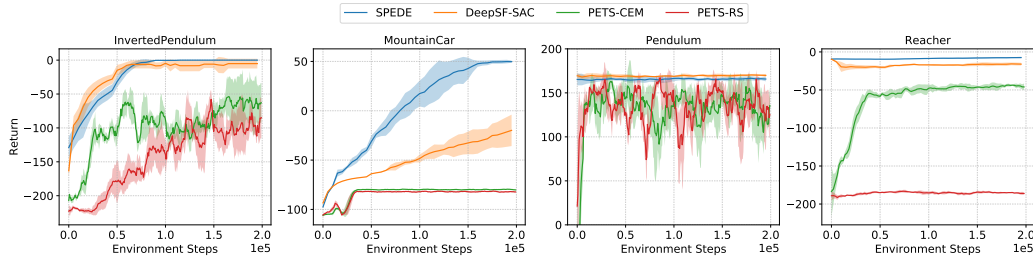


Figure 1: **Experiments on MuJoCo:** We show curves of the return versus the training steps for SPEDE and model-based RL baselines. Results show that in these tasks, our method enjoys better sample efficiency even compared to SoTA empirical model-based RL baselines.

Discussion of the Results We observe that in the environments with relatively simple dynamics (top row of Table 1), SPEDE achieves the SoTA among all the model-based and model-free RL algorithms. When the model dynamics of the environment become harder (bottom row of Table 1), the difference of the performance between the two approaches begin to enlarge. Interestingly, our SPEDE achieves strong results comparing to model-based approaches, while the joint learning SPEDE-REG outperforms model-free algorithm by a huge margin. The performance promotion of SPEDE indicates the importance on learning a good representation based on model dynamics and again shows the effectiveness of our approach in both settings. The performance gap might be caused by random feature approximation. To mitigate such approximation error, we also tried using MLP upon the learned representation, instead of linear form, which leads to better performances. Please refer to Appendix E.3 for details.

In fact, the differences in the SoTA usage of SPEDE in easy environments and difficult environments also reveals the important direction for our future work. The current rigorous representation learning methods, *e.g.*, Du et al. [2019], Misra et al. [2020], Agarwal et al. [2020a] and the proposed SPEDE, all rely on some model assumption. When the assumptions are satisfied, *e.g.*, Pendulum, Reacher, and others, our theoretically derived SPEDE variant works extremely well, even better than current SoTA. However, when the assumption is not fully satisfied, although the decoupled SPEDE achieves best performance among existing model-based RL and representation learning under fair comparison, the joint learned variant of SPEDE is more robust and promotes the current SoTA with significant margin. An interesting question is whether we can rigorously justify the regularized SPEDE, which we leave as our future work.

6 CONCLUSION

We introduce SPEDE, which, to the best of our knowledge, is the first provable and efficient representation learning algorithm for RL, by exploiting the benefits from noise. We provide thorough theoretical analysis and strong empirical

results, comparing to both model-free and model based RL, that demonstrates the effectiveness of our algorithm.

ACKNOWLEDGEMENT

Cs. Sz. greatly acknowledges funding from NSERC, AMII and the Canada CIFAR AI Chair program. This project occurred under the Google-BAIR Commons at UC Berkeley.

References

- Yasin Abbasi-Yadkori and Csaba Szepesvári. Regret bounds for the adaptive control of linear quadratic systems. In *COLT*. PMLR, 2011.
- Alekh Agarwal, Sham Kakade, Akshay Krishnamurthy, and Wen Sun. Flambe: Structural complexity and representation learning of low rank mdps. *arXiv preprint arXiv:2006.10814*, 2020a.
- Alekh Agarwal, Sham M Kakade, Jason D Lee, and Gaurav Mahajan. Optimality and approximation with policy gradient methods in markov decision processes. In *COLT*. PMLR, 2020b.
- Mauricio A Álvarez, Lorenzo Rosasco, and Neil D Lawrence. Kernels for vector-valued functions: A review. *Foundations and Trends® in Machine Learning*, 2012.
- András Antos, Csaba Szepesvári, and Rémi Munos. Fitted q-iteration in continuous action-space mdps. In *NeurIPS*, 2008.
- Nachman Aronszajn. Theory of reproducing kernels. *Transactions of the AMS*, 1950.
- Mohammad Gheshlaghi Azar, Ian Osband, and Rémi Munos. Minimax regret bounds for reinforcement learning. In *ICML*. PMLR, 2017.
- Yoshua Bengio, Aaron Courville, and Pascal Vincent. Representation learning: A review and new perspectives. *IEEE TPAMI*, 2013.

- David M Blei, Alp Kucukelbir, and Jon D McAuliffe. Variational inference: A review for statisticians. *JASA*, 2017.
- Greg Brockman, Vicki Cheung, Ludwig Pettersson, Jonas Schneider, John Schulman, Jie Tang, and Wojciech Zaremba. Openai gym, 2016.
- Xiang Cheng and Peter Bartlett. Convergence of langevin mcmc in kl-divergence. In *ALT*. PMLR, 2018.
- Kurtland Chua, Roberto Calandra, Rowan McAllister, and Sergey Levine. Deep reinforcement learning in a handful of trials using probabilistic dynamics models. *arXiv preprint arXiv:1805.12114*, 2018.
- Ignasi Clavera, Jonas Rothfuss, John Schulman, Yasuhiro Fujita, Tamim Asfour, and Pieter Abbeel. Model-based reinforcement learning via meta-policy optimization. In *CoRL*. PMLR, 2018.
- Alon Cohen, Tomer Koren, and Yishay Mansour. Learning linear-quadratic regulators efficiently with only \sqrt{t} regret. In *ICML*. PMLR, 2019.
- Bo Dai, Bo Xie, Niao He, Yingyu Liang, Anant Raj, Maria-Florina F Balcan, and Le Song. Scalable kernel methods via doubly stochastic gradients. In *NeurIPS*, 2014.
- Bo Dai, Albert Shaw, Lihong Li, Lin Xiao, Niao He, Zhen Liu, Jiانشu Chen, and Le Song. Sbeed: Convergent reinforcement learning with nonlinear function approximation. In *ICML*. PMLR, 2018.
- Varsha Dani, Thomas P Hayes, and Sham M Kakade. Stochastic linear optimization under bandit feedback. In *COLT*, 2008.
- Peter Dayan. Improving generalization for temporal difference learning: The successor representation. *Neural Computation*, 1993.
- Simon Du, Akshay Krishnamurthy, Nan Jiang, Alekh Agarwal, Miroslav Dudik, and John Langford. Provably efficient rl with rich observations via latent state decoding. In *ICML*. PMLR, 2019.
- Yaqi Duan, Zheng Tracy Ke, and Mengdi Wang. State aggregation learning from markov transition data. *arXiv preprint arXiv:1811.02619*, 2018.
- Norm Ferns, Prakash Panangaden, and Doina Precup. Metrics for finite markov decision processes. In *UAI*, 2004.
- Carles Gelada, Saurabh Kumar, Jacob Buckman, Ofir Nachum, and Marc G Bellemare. Deepmdp: Learning continuous latent space models for representation learning. In *ICML*. PMLR, 2019.
- Geoffrey Grimmett and David Stirzaker. *Probability and random processes*. Oxford university press, 2020.
- Tuomas Haarnoja, Aurick Zhou, Pieter Abbeel, and Sergey Levine. Soft actor-critic: Off-policy maximum entropy deep reinforcement learning with a stochastic actor. In *ICML*. PMLR, 2018.
- Danijar Hafner, Timothy Lillicrap, Ian Fischer, Ruben Villegas, David Ha, Honglak Lee, and James Davidson. Learning latent dynamics for planning from pixels. In *ICML*. PMLR, 2019.
- Thomas Jaksch, Ronald Ortner, and Peter Auer. Near-optimal regret bounds for reinforcement learning. *JMLR*, 2010.
- Chi Jin, Zeyuan Allen-Zhu, Sebastien Bubeck, and Michael I Jordan. Is q-learning provably efficient? In *NeurIPS*, 2018.
- Chi Jin, Praneeth Netrapalli, Rong Ge, Sham M Kakade, and Michael I Jordan. A short note on concentration inequalities for random vectors with subgaussian norm. *arXiv preprint arXiv:1902.03736*, 2019.
- Chi Jin, Zhuoran Yang, Zhaoran Wang, and Michael I Jordan. Provably efficient reinforcement learning with linear function approximation. In *COLT*. PMLR, 2020.
- Sham Kakade, Akshay Krishnamurthy, Kendall Lowrey, Motoya Ohnishi, and Wen Sun. Information theoretic regret bounds for online nonlinear control. *arXiv preprint arXiv:2006.12466*, 2020.
- Tejas D Kulkarni, Ardavan Saeedi, Simanta Gautam, and Samuel J Gershman. Deep successor reinforcement learning. *arXiv preprint arXiv:1606.02396*, 2016.
- Thanard Kurutach, Ignasi Clavera, Yan Duan, Aviv Tamar, and Pieter Abbeel. Model-ensemble trust-region policy optimization. *arXiv preprint arXiv:1802.10592*, 2018.
- Sergey Levine, Chelsea Finn, Trevor Darrell, and Pieter Abbeel. End-to-end training of deep visuomotor policies. *JMLR*, 2016.
- Sridhar Mahadevan and Mauro Maggioni. Proto-value functions: A laplacian framework for learning representation and control in markov decision processes. *JMLR*, 2007.
- Horia Mania, Stephen Tu, and Benjamin Recht. Certainty equivalence is efficient for linear quadratic control. In *NeurIPS*, 2019.
- Horia Mania, Michael I Jordan, and Benjamin Recht. Active learning for nonlinear system identification with guarantees. *arXiv preprint arXiv:2006.10277*, 2020.
- Dipendra Misra, Mikael Henaff, Akshay Krishnamurthy, and John Langford. Kinematic state abstraction and provably efficient rich-observation reinforcement learning. In *ICML*. PMLR, 2020.

- Volodymyr Mnih, Koray Kavukcuoglu, David Silver, Alex Graves, Ioannis Antonoglou, Daan Wierstra, and Martin Riedmiller. Playing atari with deep reinforcement learning. *arXiv preprint arXiv:1312.5602*, 2013.
- Aditya Modi, Jinglin Chen, Akshay Krishnamurthy, Nan Jiang, and Alekh Agarwal. Model-free representation learning and exploration in low-rank mdps. *arXiv preprint arXiv:2102.07035*, 2021.
- Ofir Nachum and Mengjiao Yang. Provable representation learning for imitation with contrastive fourier features. *arXiv preprint arXiv:2105.12272*, 2021.
- Ofir Nachum, Mohammad Norouzi, Kelvin Xu, and Dale Schuurmans. Bridging the gap between value and policy based reinforcement learning. *arXiv preprint arXiv:1702.08892*, 2017.
- Radford M Neal et al. Mcmc using hamiltonian dynamics. *Handbook of markov chain monte carlo*, 2011.
- Ian Osband and Benjamin Van Roy. Model-based reinforcement learning and the eluder dimension. In *NeurIPS*, 2014.
- Martin L Puterman. *Markov decision processes: discrete stochastic dynamic programming*. John Wiley & Sons, 2014.
- Ali Rahimi and Benjamin Recht. Random features for large-scale kernel machines. In *NeurIPS*, 2007.
- Walter Rudin. *Fourier analysis on groups*. Courier Dover Publications, 2017.
- Daniel Russo and Benjamin Van Roy. Eluder dimension and the sample complexity of optimistic exploration. *NeurIPS*, 2013.
- Daniel Russo and Benjamin Van Roy. Learning to optimize via posterior sampling. *Mathematics of Operations Research*, 2014.
- David Silver, Julian Schrittwieser, Karen Simonyan, Ioannis Antonoglou, Aja Huang, Arthur Guez, Thomas Hubert, Lucas Baker, Matthew Lai, Adrian Bolton, et al. Mastering the game of go without human knowledge. *nature*, 2017.
- Max Simchowitz and Dylan Foster. Naive exploration is optimal for online lqr. In *ICML*. PMLR, 2020.
- Richard S Sutton. Integrated architectures for learning, planning, and reacting based on approximating dynamic programming. In *Machine learning proceedings 1990*. Elsevier, 1990.
- Richard S Sutton and Andrew G Barto. *Reinforcement learning: An introduction*. MIT press, 2018.
- Masatoshi Uehara, Xuezhou Zhang, and Wen Sun. Representation learning for online and offline rl in low-rank mdps. *arXiv preprint arXiv:2110.04652*, 2021.
- Martin J Wainwright. *High-dimensional statistics: A non-asymptotic viewpoint*. Cambridge University Press, 2019.
- Ruosong Wang, Russ R Salakhutdinov, and Lin Yang. Reinforcement learning with general value function approximation: Provably efficient approach via bounded eluder dimension. In *NeurIPS*, 2020.
- Tingwu Wang, Xuchan Bao, Ignasi Clavera, Jerrick Hoang, Yeming Wen, Eric Langlois, Shunshi Zhang, Guodong Zhang, Pieter Abbeel, and Jimmy Ba. Benchmarking model-based reinforcement learning. *arXiv preprint arXiv:1907.02057*, 2019.
- Max Welling and Yee W Teh. Bayesian learning via stochastic gradient langevin dynamics. In *ICML*, 2011.
- Yifan Wu, George Tucker, and Ofir Nachum. The laplacian in rl: Learning representations with efficient approximations. *arXiv preprint arXiv:1810.04586*, 2018.
- Lin Yang and Mengdi Wang. Sample-optimal parametric q-learning using linearly additive features. In *International Conference on Machine Learning*, pages 6995–7004. PMLR, 2019.
- Lin Yang and Mengdi Wang. Reinforcement learning in feature space: Matrix bandit, kernels, and regret bound. In *ICML*. PMLR, 2020.
- Anru Zhang and Mengdi Wang. Spectral state compression of markov processes. *IEEE TIT*, 2019.
- Tianjun Zhan Zhang, Tongzheng Ren, Mengjiao Yang, Joseph Gonzalez, Dale Schuurmans, and Bo Dai. Making linear mdps practical via contrastive representation learnin. In *ICML*. PMLR, 2022.

A BACKGROUNDS ON REPRODUCING KERNEL HILBERT SPACE

We briefly introduce the basic concepts of the Reproducing Kernel Hilbert Space, which is helpful on understanding our paper. To start with, we first define the inner product.

Definition 6 (Inner Product). *A function $\langle \cdot, \cdot \rangle_{\mathcal{H}} : \mathcal{H} \times \mathcal{H} \rightarrow \mathbb{R}$ is said to be an inner product on \mathcal{H} if it satisfies the following conditions:*

1. *Positive Definiteness:* $\forall u \in \mathcal{H}, \langle u, u \rangle \geq 0$, and $\langle u, u \rangle = 0 \iff u = 0$.
2. *Symmetry:* $\forall u, v \in \mathcal{H}, \langle u, v \rangle \in \langle v, u \rangle$.
3. *Bilinearity:* $\forall \alpha, \beta \in \mathbb{R}, u, v, w \in \mathcal{H}, \langle \alpha u + \beta v, w \rangle = \alpha \langle u, w \rangle + \beta \langle v, w \rangle$.

Additionally, we can define a norm with the inner product: $\|u\| = \sqrt{\langle u, u \rangle}$.

A Hilbert space is a space equipped with an inner product and satisfies an additional technical condition of completeness. The finite-dimension vector space with the canonical inner product is an example of the Hilbert space. We remark that \mathcal{H} can also be a function space, for example, the space contains all square integrable functions (i.e. $\int_{\mathbb{R}} f(x)^2 dx < \infty$, generally denoted as L_2) is also a Hilbert space with inner product $\langle f, g \rangle = \int_{\mathbb{R}} f(x)g(x) dx$.

We then define the kernel, and introduce the notion of positive-definite kernel [Álvarez et al., 2012].

Definition 7 ((Positive-Definite) Kernel). *A function $k : \mathcal{X} \times \mathcal{X} \rightarrow \mathbb{R}$ is said to be a kernel on non-empty set \mathcal{X} if there exists a Hilbert space \mathcal{H} and a feature map $\phi : \mathcal{X} \rightarrow \mathcal{H}$ such that $\forall x, x' \in \mathcal{X}$, we have*

$$k(x, x') = \langle \phi(x), \phi(x') \rangle_{\mathcal{H}}.$$

Moreover, the kernel is said to be positive definite if $\forall n \geq 1, \forall \{a_i\}_{i \in [n]} \subset \mathbb{R}$ and mutually distinct set $\{x_i\}_{i \in [n]} \subset \mathcal{X}$, we have that

$$\sum_{i \in [n]} \sum_{j \in [n]} a_i a_j k(x_i, x_j) > 0.$$

Some well-known kernels include:

- **Linear Kernel:** $k(x, y) = \langle x, y \rangle$, with the canonical feature map $\phi(x) = x$.
- **Polynomial Kernel:** $k(x, y) = (\langle x, y \rangle + c)^m$, where $m \in \mathbb{N}^+$ and $c \in \mathbb{R}^+$.
- **Gaussian (a.k.a radial basis function, RBF) Kernel:** $k(x, y) = \exp\left(-\frac{\|x-y\|_2^2}{2\sigma^2}\right)$. It's known that such kernel is positive definite.

Now we can define the Reproducing Kernel Hilbert space (RKHS) [Aronszajn, 1950].

Definition 8 (Reproducing Kernel Hilbert Space (RKHS)). *The Hilbert space \mathcal{H} of \mathbb{R} -valued function defined on a non-empty set \mathcal{X} is said to be a reproducing kernel Hilbert space (RKHS) if there is a kernel $k : \mathcal{X} \times \mathcal{X} \rightarrow \mathbb{R}$, such that*

1. $\forall x \in \mathcal{X}, k(x, \cdot) \in \mathcal{H}$.
2. $\forall x \in \mathcal{X}, f \in \mathcal{H}, \langle f, k(x, \cdot) \rangle_{\mathcal{H}} = f(x)$ (a.k.a the reproducing property), which also implies that $\langle k(x, \cdot), k(y, \cdot) \rangle = k(x, y)$.

Here k is called a reproducing kernel of \mathcal{H} .

We provide an intuitive interpretation on the definition of RKHS when \mathcal{H} is the space of linear function. Consider $\mathcal{X} = \mathbb{R}^d$ and $k(x, y) = \langle x, y \rangle$. With the definition of the kernel k , we can see that $k(x, \cdot) : \mathcal{X} \rightarrow \mathbb{R}$ is a linear function, and thus lies in \mathcal{H} . Meanwhile, $\forall f \in \mathcal{H}$, there exists θ_f such that $f(x) = \theta_f^\top x$. We define the inner product on \mathcal{H} via $\langle f, g \rangle_{\mathcal{H}} = \langle \theta_f, \theta_g \rangle$, and thus $\langle f, k(x, \cdot) \rangle_{\mathcal{H}} = \theta_f^\top x = f(x)$, which demonstrates the reproducing property, and shows that the space of linear function on any finite-dimensional vector space is an RKHS with linear kernel as the corresponding reproducing kernel.

We state the following theorems without the proof.

Theorem 9 (Moore-Aronszajn [Aronszajn, 1950]). *Every positive definite kernel k is associated with a unique RKHS \mathcal{H} .*

Notice that, Moore-Aronszajn theorem guarantees that all of the positive kernel can be represented as the inner product in certain Hilbert space, hence we can have a linear representation of the Gaussian distribution induced by the reproducing property of Gaussian kernel, as we illustrated in the main text.

Theorem 10 (Bochner [Rudin, 2017]). *A continuous, shift-invariant kernel (i.e. $k(x, y) = k(x - y)$) is positive definite if and only if $k(x - y)$ is the Fourier transform of a non-negative measure ω , i.e.*

$$k(x - y) = \int_{\mathbb{R}^d} \exp(i\omega^\top(x - y)) d\mathbb{P}(\omega) = \int_{\mathbb{R}^d \times [0, 2\pi]} 2 \cos(\omega^\top x + b) \cos(\omega^\top y + b) d(\mathbb{P}(\omega) \times \mathbb{P}(b)),$$

where $\mathbb{P}(b)$ is a uniform distribution on $[0, 2\pi]$.

Bochner's theorem shows that any continuous positive definite shift-invariant kernel (e.g. Gaussian kernel, Laplacian kernel) can be represented as the inner product of random Fourier feature, which provides an additional way to provide a representation for certain distribution [see Rahimi and Recht, 2007, Dai et al., 2014].

B AN EQUIVALENT UPPER CONFIDENCE BOUND ALGORITHM

In this section, we provide a generic Upper Confidence Bound (UCB) algorithm with the OFU principle, and show the connections and differences between the UCB algorithm and the TS algorithm. The prototype for our UCB algorithm is illustrated in Algorithm 3.

Algorithm 3 Upper Confidence Bound (UCB) Algorithm

Require: Number of Episodes K , Failure Probability $\delta \in (0, 1)$, Reward Function $r(s, a)$.

1: Initialize the history set $\mathcal{H}_0 = \emptyset$.

2: **for** episodes $k = 1, 2, \dots$ **do**

3: **Compute** π_k **via**

▷ Optimistic Planning.

$$(\pi_k, \tilde{f}_k) = \arg \max_{\pi \in \Pi, f \in \mathcal{F}_k} \tilde{V}_0^\pi(s_0).$$

where \mathcal{F}_k is defined in (10).

4: **for** steps $h = 0, 1, \dots, H - 1$ **do**

▷ Execute π_k .

5: Execute $a_h^k \sim \pi_k^h(s_h^k)$.

6: Observe s_{h+1} .

7: **end for**

8: Set $\mathcal{H}_k = \mathcal{H}_{k-1} \cup \{(s_h^k, a_h^k, s_{h+1}^k)\}_{h=0}^{H-1}$.

▷ Update the History.

9: **end for**

Notice that, the only difference between UCB algorithm and TS algorithm is the mechanism of finding f we use to plan for each episode (highlighted in blue). For UCB algorithm, we perform an optimistic planning, which finds the \tilde{f}_k that potentially has the largest cumulative reward. However, such constrained optimization problem is NP-hard even for the simplest linear bandits [Dani et al., 2008]. Instead, for TS algorithm, we only sample the f_k from the posterior distribution, which gets rid of the complicated constraint optimization. We are interested in the UCB algorithm, as the worst case regret bound of the UCB algorithm can be directly translated to the expected regret bound of the TS algorithm without the need of explicit manipulation of the prior and the posterior [Russo and Van Roy, 2013, 2014, Osband and Van Roy, 2014].

Confidence Set Construction Perhaps the most important part in OFU-style algorithm is the construction of confidence set \mathcal{F}_k . To enable sample-efficient learning, the confidence set should

1. contain f^* with high probability, so that we can identify f^* eventually;
2. shrink as fast as possible, so that we can identify f^* efficiently.

In the tabular setting, \mathcal{F}_k is constructed via the concentration of sub-Gaussian/sub-Gamma random variable [e.g. Azar et al., 2017], and in the linear MDP setting, \mathcal{F}_k is constructed via the concentration on the linear parameters. As we don't assume any specific structures, we instead constructed \mathcal{F}_k via the concentration on the ℓ_2 error, following the idea of [Russo and Van Roy, 2013, Osband and Van Roy, 2014]. Specifically, consider the least-square estimates defined by

$$\hat{f}_K = \arg \min_{f \in \mathcal{F}} L_{2,K}(f) := \sum_{k \in [K]} \sum_{h=0}^{H-1} \|f(s_h^k, a_h^k) - s_{h+1}^k\|_2^2. \quad (9)$$

As $s_{h+1}^k = f^*(s_h^k, a_h^k) + \epsilon_h^k$ where ϵ_h^k is the Gaussian noise added to the step h at the k -th episode, we know \hat{f}_K will not deviate from f^* a lot. Meanwhile, as K increases, the estimation \hat{f}_K should become closer to f^* . Specifically, define the empirical 2-norm $\|\cdot\|_{2,E_t}$ as

$$\|g\|_{2,E_K}^2 := \sum_{k \in [K]} \sum_{h=0}^{H-1} \|g(s_h^k, a_h^k)\|_2^2.$$

We can construct the confidence set based on the following lemma:

Lemma 11 (Confidence Set Construction [Russo and Van Roy, 2013, Osband and Van Roy, 2014]). *Define*

$$\mathcal{F}_K = \left\{ f \in \mathcal{F} : \|f - \hat{f}_K\|_{2,E_K} \leq \sqrt{\beta_K^*(\mathcal{F}, \delta, \alpha)} \right\}, \quad (10)$$

then

$$\mathbb{P}_{f^*} \left(f^* \in \bigcap_{k=1}^{\infty} \mathcal{F}_k \right) \geq 1 - 2\delta, \quad (11)$$

where

$$\beta_K^*(\mathcal{F}, \delta, \alpha) = 8\sigma^2 \log(\mathcal{N}(\mathcal{F}, \alpha, \|\cdot\|_2)/\delta) + 2H\alpha(12C + \sqrt{8d\sigma^2 \log(4K^2H/\delta)}). \quad (12)$$

The proof can be found in Appendix C.1. Notice that, the empirical 2-norm $\|f - \hat{f}_K\|_{2,E_K}$ scales linearly with K , and $\beta_K^*(\mathcal{F}, \delta, \alpha)$ only scales as $\log K$, so the confidence set shrinks. Meanwhile, Equation 11 guarantees that $f^* \in \mathcal{F}_k, \forall k$ with high probability. Hence, it satisfies our requirement for the confidence set.

Regret Upper Bound We have the following upper bound of the regret for the UCB algorithm:

Theorem 12 (Regret Bound). *Assume Assumption 2 to 5 holds. We have that*

$$\text{Regret}(K) \leq \tilde{O}(\sqrt{H^2 T \cdot \log \mathcal{N}(\mathcal{F}, T^{-1/2}, \|\cdot\|_2) \cdot \dim_E(\mathcal{F}, T^{-1/2})}).$$

where \tilde{O} represents the order up to logarithm factors.

C TECHNICAL PROOF

C.1 PROOF FOR LEMMA 11

Proof. We first show the following concentration on the ℓ_2 error:

Lemma 13 (Concentration of ℓ_2 error [Russo and Van Roy, 2013, Osband and Van Roy, 2014, Wang et al., 2020]). $\forall \delta > 0, f : \mathcal{S} \times \mathcal{A} \rightarrow \mathbb{R}$, we have

$$\mathbb{P}_{f^*} \left(L_{2,K}(f) \geq L_{2,K}(f^*) + \frac{1}{2} \|f - f^*\|_{2,E_K}^2 - 4\sigma^2 \log(1/\delta), \quad \forall K \in \mathbb{N} \right) \geq 1 - \delta$$

Proof. Define the filtration $\mathcal{H}_{k,h} = \{(s_h^i, a_h^i)\}_{i \in [k-1], h=0, \dots, H-1} \cup \{(s_h^k, a_h^k)\}_{h=0}^{h-1}$, and the random variable $Z_{k,h}$ adapted to the filtration $\mathcal{H}_{k,h}$ via:

$$\begin{aligned} Z_{k,h} &= \|f^*(s_h^k, a_h^k) - s_{h+1}^k\|_2^2 - \|f(s_h^k, a_h^k) - s_{h+1}^k\|_2^2 \\ &= \|f^*(s_h^k, a_h^k) - s_{h+1}^k\|_2^2 - \|f(s_h^k, a_h^k) - f^*(s_h^k, a_h^k) + f^*(s_h^k, a_h^k) - s_{h+1}^k\|_2^2 \\ &= -\|f(s_h^k, a_h^k) - f^*(s_h^k, a_h^k)\|_2^2 + 2\langle f(s_h^k, a_h^k) - f^*(s_h^k, a_h^k), \epsilon_h^k \rangle, \end{aligned}$$

where $\epsilon_h^k = s_{h+1}^k - f^*(s_h^k, a_h^k)$. Thus, $\mathbb{E}(Z_k^h | \mathcal{H}_{k,h}) = -\|f(s_h^k, a_h^k) - f^*(s_h^k, a_h^k)\|_2^2$, and $Z_k^h + \|f(s_h^k, a_h^k) - f^*(s_h^k, a_h^k)\|_2^2$ is a martingale w.r.t $\mathcal{H}_{k,h}$. Notice that we assume ϵ is an isotropic Gaussian noise with variance σ^2 on each of the dimension, thus the conditional moment generating function of $Z_k^h + \|f(s_h^k, a_h^k) - f^*(s_h^k, a_h^k)\|_2^2$ satisfies:

$$\begin{aligned} M_{k,h}(\lambda) &= \log \mathbb{E}[\exp(\lambda(Z_k^h + \|f(s_h^k, a_h^k) - f^*(s_h^k, a_h^k)\|_2^2)) | \mathcal{H}_{k,h}] \\ &= \log \mathbb{E}[\exp(\langle 2\lambda f(s_h^k, a_h^k) - f^*(s_h^k, a_h^k), \epsilon_h^k \rangle) | \mathcal{H}_{k,h}] \\ &\leq 2\sigma^2 \lambda^2 \|f(s_h^k) - f^*(s_h^k, a_h^k)\|_2^2. \end{aligned}$$

Applying Lemma 4 in [Russo and Van Roy, 2013], we have that, $\forall x, \lambda \geq 0$,

$$\mathbb{P}_{f^*} \left(\sum_{k \in [K]} \sum_{h=0}^{H-1} \lambda Z_{k,h} \leq x - \lambda(1 - 2\lambda\sigma^2) \sum_{k \in [K]} \sum_{h=0}^{H-1} \|f(s_h^k, a_h^k) - f^*(s_h^k, a_h^k)\|_2^2, \quad \forall k \in \mathbb{N} \right) \leq 1 - \exp(-x).$$

Take $\lambda = \frac{1}{4\sigma^2}$, $x = \log 1/\delta$, and notice that $\sum_{k \in [K]} \sum_{h=0}^{H-1} Z_{k,h} = L_{2,K}(f^*) - L_{2,K}(f)$, we have the desired result. \square

We construct an α -cover \mathcal{F}_α in \mathcal{F} with respect to $\|\cdot\|_2$. With a standard union bound, we know that condition on f^* , with probability at least $1 - \delta$, we have that

$$L_{2,K}(f^\alpha) - L_{2,K}(f^*) \geq \frac{1}{2} \|f^\alpha - f^*\|_{2,E_K}^2 - 4\sigma^2 \log(|F^\alpha|/\delta), \quad \forall K \in \mathbb{N}, f^\alpha \in \mathcal{F}^\alpha.$$

Thus, we have that

$$\begin{aligned} L_{2,K}(f) - L_{2,K}(f^*) &\geq \frac{1}{2} \|f - f^*\|_{2,E_K}^2 - 4\sigma^2 \log(|F^\alpha|/\delta) \\ &\quad + \underbrace{\min_{f^\alpha \in \mathcal{F}^\alpha} \left\{ \frac{1}{2} \|f^\alpha - f^*\|_{2,E_K}^2 - \frac{1}{2} \|f - f^*\|_{2,E_K}^2 + L_{2,K}(f) - L_{2,K}(f^\alpha) \right\}}_{\text{Discretization Error}}. \end{aligned}$$

We then deal with the discretization error. Assume $\alpha \leq 2C$ (or otherwise we only have a trivial cover) and $\|f^\alpha(s, a) - f(s, a)\|_2 \leq \alpha$, we have that

$$\begin{aligned} &\|f^\alpha(s, a) - f^*(s, a)\|_2^2 - \|f(s, a) - f^*(s, a)\|_2^2 \\ &= \|f^\alpha(s, a)\|_2^2 - \|f(s, a)\|_2^2 + 2\langle f^*(s, a), f(s, a) - f^\alpha(s, a) \rangle \\ &\leq \max_{\|y\|_2 \leq \alpha} \{ \|f(s, a) + y\|_2^2 - \|f(s, a)\|_2^2 \} + 2C\alpha \\ &= \max_{\|y\|_2 \leq \alpha} \{ 2\langle f(s, a), y \rangle + \|y\|_2^2 \} + 2C\alpha \\ &\leq 4C\alpha + \alpha^2 \leq 6C\alpha, \end{aligned}$$

where the inequality is by Cauchy-Schwartz inequality and $\alpha \leq 2C$. Meanwhile,

$$\begin{aligned} &\|s' - f(s, a)\|_2^2 - \|s' - f^\alpha(s, a)\|_2^2 \\ &= 2\langle s', f^\alpha(s, a) - f(s, a) \rangle + \|f(s, a)\|_2^2 - \|f^\alpha(s, a)\|_2^2 \\ &\leq 2\langle \epsilon, f^\alpha(s, a) - f(s, a) \rangle + 2\langle f^*(s, a), f^\alpha(s, a) - f(s, a) \rangle + 2C\alpha + \alpha^2 \\ &\leq 2\|\epsilon\|_2 \alpha + 6C\alpha. \end{aligned}$$

We now consider the concentration property of $\|\epsilon\|_2$. Here we simply follow [Jin et al., 2019] and notice that ϵ is $\sqrt{d\sigma}$ -norm-sub-Gaussian, we have that

$$\mathbb{P}(\|\epsilon\|_2 > \sqrt{2d\sigma^2 \log(2/\delta)}) \leq \delta.$$

By a union bound, we have that

$$\mathbb{P}(\exists k, \|\epsilon\|_2 > \sqrt{2d\sigma^2 \log(4k^2 H/\delta)}) \leq \frac{\delta}{2} \sum_{k=1}^{\infty} \sum_{h=0}^{H-1} \frac{1}{k^2 H} \leq \delta.$$

Sum all these up, we can see with probability $1 - \delta$, $\forall K \in \mathbb{N}$, the discretization error is upper bounded by:

$$H\alpha(12C + \sqrt{8d\sigma^2 \log(4K^2 H/\delta)}).$$

As we consider the least square estimate \hat{f}_K , we have that $L_{2,K}(\hat{f}_K) - L_{2,K}(f^*) \leq 0$. Substitute back, we have the desired results. \square

C.2 SIMULATION LEMMA

Lemma 14 (Simulation Lemma (adapted from Lemma 3.9 in [Kakade et al., 2020])). *Given \hat{f} , $\forall s \in \mathcal{S}$, the value function \hat{V}^π and V^π corresponding to the model \hat{f} and f^* satisfies*

$$\hat{V}_0^\pi(s) - V_0^\pi(s) \leq H^{3/2} \sqrt{\mathbb{E} \left[\sum_{h=0}^{H-1} \min \left\{ \frac{2\|f^*(s_h, a_h) - \hat{f}(s_h, a_h)\|_2^2}{\sigma^2}, 1 \right\} \right]}.$$

Proof. We first show the following difference lemma:

Lemma 15 (Difference Lemma). *Assume the trajectory $\{(s_h, a_h)\}_{h=0}^{H-1}$ is generated via policy π and ground truth f^* , define*

$$V_h = \sum_{\tau=h}^{H-1} r(s_\tau, a_\tau)$$

then $\forall \tau \in \{1, \dots, H-1\}$, we have:

$$\begin{aligned} \hat{V}_0^\pi(s_0) - V_0 &= \mathbb{E}_{s'_\tau \sim \mathcal{N}(\hat{f}(s_{\tau-1}, a_{\tau-1}), \sigma^2 I)} \left[\hat{V}_\tau^\pi(s'_\tau) \right] - V_\tau \\ &\quad + \sum_{h=1}^{\tau-1} \left[\mathbb{E}_{s'_h \sim \mathcal{N}(f(s_{h-1}, a_{h-1}), \sigma^2 I)} \left[\hat{V}_h^\pi(s'_h) \right] - \hat{V}_h^\pi(s_h) \right]. \end{aligned}$$

Proof. When $\tau = 1$, we can obtain the result with $a_0 = \pi(s_0)$ and

$$\hat{V}_0^\pi(s_0) = r(s_0, \pi(s_0)) + \mathbb{E}_{s'_1 \sim \mathcal{N}(f(s_0, a_0), \sigma^2 I)} \hat{V}_1^\pi(s'_1).$$

We only need to show the case when $\tau = 2$, and the case when $\tau > 2$ can be derived via recursion. Notice that

$$\begin{aligned} \hat{V}_0^\pi(s_0) - V_0 &= \mathbb{E}_{s'_1 \sim \mathcal{N}(f(s_0, a_0), \sigma^2 I)} \left[\hat{V}_1^\pi(s'_1) \right] - V_1 \\ &= \hat{V}_1^\pi(s_1) - V_1 + \mathbb{E}_{s'_1 \sim \mathcal{N}(f(s_0, a_0), \sigma^2 I)} \left[\hat{V}_1^\pi(s'_1) \right] - \hat{V}_1^\pi(s_1) \\ &= \mathbb{E}_{s'_2 \sim \mathcal{N}(f(s_1, a_1), \sigma^2 I)} \left[\hat{V}_2^\pi(s'_2) \right] - V_2 + \mathbb{E}_{s'_1 \sim \mathcal{N}(f(s_0, a_0), \sigma^2 I)} \left[\hat{V}_1^\pi(s'_1) \right] - \hat{V}_1^\pi(s_1), \end{aligned}$$

where the last equality is due to the fact that $a_1 = \pi(s_1)$. \square

We then follow the idea of “optional stopping” used in [Kakade et al., 2020] and show the following “optional stopping” simulation lemma.

Lemma 16 (“Optional Stopping” Simulation Lemma). *Consider the stochastic process over the trajectories $\{(s_h, a_h)\}_{h=0}^{H-1}$ generated via policy π and ground truth f^* , where the randomness is from the Gaussian noise in the dynamics. Define a stopping time τ w.r.t this stochastic process and a given model \hat{f} via:*

$$\tau := \min\{h \geq 0 : \hat{V}_h^\pi(s_h) \leq V_h^\pi(s_h)\}.$$

Furthermore, define a random variable:

$$\tilde{V}_h^\pi(s_h) = \max\{\hat{V}_h^\pi(s_h), V_h^\pi(s_h)\},$$

we have that

$$\hat{V}_0^\pi(s_0) - V_0^\pi(s_0) \leq \mathbb{E} \left[\sum_{h=0}^{H-1} \mathbf{1}_{h < \tau} \left(\mathbb{E}_{s'_{h+1} \sim \mathcal{N}(f^*(s_h, a_h), \sigma^2 I)} \tilde{V}_h^\pi(s'_{h+1}) - \mathbb{E}_{s'_{h+1} \sim \mathcal{N}(\hat{f}(s_h, a_h), \sigma^2 I)} \tilde{V}_h^\pi(s'_{h+1}) \right) \right],$$

where the expectation is w.r.t the stochastic process over the trajectories.

Proof. Define the filtration $\mathcal{F}_h := \{\epsilon_i\}_{i=0}^{h-1}$, where ϵ_i is the noise that add to the dynamics at step i . Define

$$M_h = \mathbb{E}[\hat{V}_0^\pi(s_0) - V_0 | \mathcal{F}_h],$$

which is a Doob martingale with respect to \mathcal{F}_i [Grimmett and Stirzaker, 2020]. As $\tau \leq H$, by Doob’s optional stopping theorem, we have that

$$\mathbb{E}[\hat{V}_0^\pi(s_0) - V_0] = \mathbb{E}[M_\tau] = \mathbb{E}[\mathbb{E}[\hat{V}_0^\pi(s_0) - V_0 | \mathcal{F}_\tau]].$$

We then provide a bound for M_τ . By Lemma 15, we have that

$$\begin{aligned} M_\tau &= \mathbb{E}[\hat{V}_0^\pi(s_0) - V_0 | \mathcal{F}_\tau] \\ &= \mathbb{E}_{s'_\tau \sim \mathcal{N}(\hat{f}(s_{\tau-1}, a_{\tau-1}), \sigma^2 I)} [\hat{V}_\tau^\pi(s'_\tau)] - V_\tau^\pi(s_\tau) \\ &\quad + \mathbb{E}_{s'_h \sim \mathcal{N}(\hat{f}(s_{h-1}, a_{h-1}), \sigma^2 I)} [\hat{V}_h^\pi(s'_h)] - \sum_{h=1}^{\tau-1} \hat{V}_h^\pi(s_h) \\ &= \sum_{h=1}^{\tau} \left(\mathbb{E}_{s'_h \sim \mathcal{N}(\hat{f}(s_h, a_h), \sigma^2)} [\hat{V}_h^\pi(s'_h)] - \tilde{V}_h^\pi(s_h) \right) \\ &\leq \sum_{h=1}^{\tau} \left(\mathbb{E}_{s'_h \sim \mathcal{N}(\hat{f}(s_h, a_h), \sigma^2 I)} [\tilde{V}_h^\pi(s_h)] - \tilde{V}_h^\pi(s_h) \right) \\ &= \sum_{h=1}^H \mathbf{1}_{h \leq \tau} \left(\mathbb{E}_{s'_h \sim \mathcal{N}(\hat{f}(s_h, a_h), \sigma^2 I)} [\tilde{V}_h^\pi(s_h)] - \tilde{V}_h^\pi(s_h) \right), \end{aligned}$$

where the third inequality follows the definition of τ (and thus $V_\tau^\pi(s_\tau) = \tilde{V}_\tau^\pi(s_\tau)$ and $\hat{V}_h^\pi(s_h) = \tilde{V}_h^\pi(s_h)$ for $h < \tau$.)

The proof is then concluded via the following observation:

$$\begin{aligned} &\mathbb{E} \left[\mathbf{1}_{h \leq \tau} \left(\mathbb{E}_{s'_h \sim \mathcal{N}(\hat{f}(s_h, a_h), \sigma^2 I)} [\tilde{V}_h^\pi(s_h)] - \tilde{V}_h^\pi(s_h) \right) \right] \\ &= \mathbb{E} \left[\mathbb{E} \left[\mathbf{1}_{h \leq \tau} \left(\mathbb{E}_{s'_h \sim \mathcal{N}(\hat{f}(s_h, a_h), \sigma^2 I)} [\tilde{V}_h^\pi(s_h)] - \tilde{V}_h^\pi(s_h) \right) \middle| \mathcal{F}_{h-1} \right] \right] \\ &= \mathbb{E} \left[\mathbb{E} \left[\mathbf{1}_{h-1 < \tau} \left(\mathbb{E}_{s'_h \sim \mathcal{N}(\hat{f}(s_h, a_h), \sigma^2 I)} [\tilde{V}_h^\pi(s_h)] - \tilde{V}_h^\pi(s_h) \right) \middle| \mathcal{F}_{h-1} \right] \right] \\ &= \mathbb{E} \left[\mathbf{1}_{h-1 < \tau} \mathbb{E} \left[\left(\mathbb{E}_{s'_h \sim \mathcal{N}(\hat{f}(s_h, a_h), \sigma^2 I)} [\tilde{V}_h^\pi(s_h)] - \tilde{V}_h^\pi(s_h) \right) \middle| \mathcal{F}_{h-1} \right] \right] \\ &= \mathbb{E} \left[\mathbf{1}_{h-1 < \tau} \left(\mathbb{E}_{s'_h \sim \mathcal{N}(\hat{f}(s_h, a_h), \sigma^2)} [\tilde{V}_h^\pi(s_h)] - \mathbb{E}_{s'_h \sim \mathcal{N}(f^*(s_h, a_h), \sigma^2)} [\tilde{V}_h^\pi(s_h)] \right) \right], \end{aligned}$$

where the third equality is due to the fact that $\mathbf{1}_{h-1 < \tau}$ is measurable under \mathcal{F}_{h-1} . □

Before we finally provide the proof of Lemma 14, we state the following lemma that bound the expectation under two isotropic Gaussian distribution with different mean:

Lemma 17 (Difference of Expectation under Different Mean Isotropic Gaussian). \forall (approximately measurable) positive function g , we have that

$$\mathbb{E}_{z \sim \mathcal{N}(\mu_1, \sigma^2 I)}[g(z)] - \mathbb{E}_{z \sim \mathcal{N}(\mu_2, \sigma^2 I)}[g(z)] \leq \min \left\{ \frac{\sqrt{2}\|\mu_1 - \mu_2\|}{\sigma}, 1 \right\} \sqrt{\mathbb{E}_{z \sim \mathcal{N}(\mu_1, \sigma^2 I)}[g(z)^2]}$$

Proof.

$$\begin{aligned} & \mathbb{E}_{z \sim \mathcal{N}(\mu_1, \sigma^2 I)}[g(z)] - \mathbb{E}_{z \sim \mathcal{N}(\mu_2, \sigma^2 I)}[g(z)] \\ &= \mathbb{E}_{z \sim \mathcal{N}(\mu_1, \sigma^2 I)} \left[g(z) \left(1 - \exp \left(\frac{2(\mu_1 - \mu_2)^\top z + \|\mu_2\|^2 - \|\mu_1\|^2}{2\sigma^2} \right) \right) \right] \\ &\leq \sqrt{\mathbb{E}_{z \sim \mathcal{N}(\mu_1, \sigma^2 I)}[g(z)^2]} \sqrt{\mathbb{E}_{z \sim \mathcal{N}(\mu_1, \sigma^2 I)} \left(1 - \exp \left(\frac{2(\mu_2 - \mu_1)^\top z - \|\mu_2\|^2 + \|\mu_1\|^2}{2\sigma^2} \right) \right)^2} \end{aligned}$$

We then calculate

$$\begin{aligned} & \mathbb{E}_{z \sim \mathcal{N}(\mu_1, \sigma^2 I)} \left(1 - \exp \left(\frac{2(\mu_2 - \mu_1)^\top z - \|\mu_2\|^2 + \|\mu_1\|^2}{2\sigma^2} \right) \right)^2 \\ &= 1 - \frac{2}{\sqrt{2\pi}\sigma^{d/2}} \int \exp \left(\frac{-\|z - \mu_1\|_2^2 + 2(\mu_2 - \mu_1)^\top z - \|\mu_2\|^2 + \|\mu_1\|^2}{2\sigma^2} \right) dz \\ &\quad + \frac{1}{\sqrt{2\pi}\sigma^{d/2}} \int \exp \left(\frac{-\|z - \mu_1\|_2^2 + 4(\mu_2 - \mu_1)^\top z - 2\|\mu_2\|^2 + 2\|\mu_1\|^2}{2\sigma^2} \right) dz \\ &= -1 + \frac{1}{\sqrt{2\pi}\sigma^{d/2}} \int \exp \left(\frac{-\|z - (2\mu_2 - \mu_1)\|_2^2 + 2\|\mu_2 - \mu_1\|_2^2}{2\sigma^2} \right) dz \\ &= -1 + \exp \left(\frac{\|\mu_2 - \mu_1\|_2^2}{\sigma^2} \right). \end{aligned}$$

Also notice that, as g is positive, a simple bound is that

$$\mathbb{E}_{z \sim \mathcal{N}(\mu_1, \sigma^2 I)}[g(z)] - \mathbb{E}_{z \sim \mathcal{N}(\mu_2, \sigma^2 I)}[g(z)] \leq \mathbb{E}_{z \sim \mathcal{N}(\mu_1, \sigma^2 I)}[g(z)] \leq \sqrt{\mathbb{E}_{z \sim \mathcal{N}(\mu_1, \sigma^2 I)}[g(z)^2]}.$$

Thus,

$$\mathbb{E}_{z \sim \mathcal{N}(\mu_1, \sigma^2 I)}[g(z)] - \mathbb{E}_{z \sim \mathcal{N}(\mu_2, \sigma^2 I)}[g(z)] \leq \sqrt{\mathbb{E}_{z \sim \mathcal{N}(\mu_1, \sigma^2 I)}[g(z)^2]} \sqrt{\min \left\{ \exp \left(\frac{\|\mu_2 - \mu_1\|_2^2}{\sigma^2} \right) - 1, 1 \right\}}.$$

Notice that, if $\|\mu_2 - \mu_1\| \geq \sigma$, then $\exp \left(\frac{\|\mu_2 - \mu_1\|_2^2}{\sigma^2} \right) - 1 \geq 1$. Meanwhile, when $x \in [0, 1]$, $\exp(x) \leq 1 + 2x$. Thus,

$$\sqrt{\min \left\{ \exp \left(\frac{\|\mu_2 - \mu_1\|_2^2}{\sigma^2} \right) - 1, 1 \right\}} \leq \sqrt{\min \left\{ 1 + \frac{2\|\mu_2 - \mu_1\|_2^2}{\sigma^2} - 1, 1 \right\}} = \min \left\{ \frac{2\|\mu_2 - \mu_1\|_2^2}{\sigma^2}, 1 \right\},$$

which finishes the proof. \square

With Lemma 16, we have that

$$\begin{aligned} & \hat{V}_0^\pi(s_0) - V_0^\pi(s_0) \\ &\leq \mathbb{E} \left[\mathbf{1}_{h-1 < \tau} \left(\mathbb{E}_{s'_h \sim \mathcal{N}(\hat{f}(s_h, a_h), \sigma^2)} \left[\tilde{V}_h^\pi(s_h) \right] - \mathbb{E}_{s'_h \sim \mathcal{N}(f^*(s_h, a_h), \sigma^2)} \left[\tilde{V}_h^\pi(s_h) \right] \right) \right] \\ &\leq \sum_{h=0}^{H-1} \mathbb{E} \left[\sqrt{\mathbb{E}_{s'_{h+1} \sim \mathcal{N}(\hat{f}(s_h, a_h), \sigma^2)} \left[\tilde{V}_h^\pi(s'_{h+1})^2 \right]} \min \left\{ \frac{\sqrt{2}\|f^*(s_h, a_h) - \hat{f}(s_h, a_h)\|_2}{\sigma}, 1 \right\} \right] \end{aligned}$$

$$\begin{aligned}
&\leq \sum_{h=0}^{H-1} \sqrt{\mathbb{E} \left[\mathbb{E}_{s'_{h+1} \sim \mathcal{N}(\hat{f}(s_h, a_h), \sigma^2)} \left[\tilde{V}_h^\pi(s'_{h+1})^2 \right] \right]} \sqrt{\mathbb{E} \left[\min \left\{ \frac{2\|f^*(s_h, a_h) - \hat{f}(s_h, a_h)\|_2^2}{\sigma^2}, 1 \right\} \right]} \\
&\leq \sqrt{\mathbb{E} \left[\sum_{h=0}^{H-1} \mathbb{E}_{s'_{h+1} \sim P(\cdot | f^*(s_h, a_h))} \left[\tilde{V}_h^\pi(s'_{h+1})^2 \right] \right]} \sqrt{\mathbb{E} \left[\sum_{h=0}^{H-1} \min \left\{ \frac{2\|f^*(s_h, a_h) - \hat{f}(s_h, a_h)\|_2^2}{\sigma^2}, 1 \right\} \right]} \\
&\leq H^{3/2} \sqrt{\mathbb{E} \left[\sum_{h=0}^{H-1} \min \left\{ \frac{2\|f^*(s_h, a_h) - \hat{f}(s_h, a_h)\|_2^2}{\sigma^2}, 1 \right\} \right]}
\end{aligned}$$

where the second inequality is due to Lemma 17, and the last inequality is due to the fact that $\tilde{V}_h^\pi(s'_{h+1}) \leq H, \forall h$. \square

C.3 SUM OF WIDTH SQUARE

Lemma 18 (Bound on the Sum of Width Square). *Define*

$$w_{\mathcal{F}}(s, a) := \sup_{\bar{f}, \underline{f} \in \mathcal{F}} \|\bar{f}(s, a) - \underline{f}(s, a)\|_2.$$

If $\{\beta_k^*\}_{k \in [K]}$ is a non-decreasing sequence, and $\|f\|_2 < C, \forall f \in \mathcal{F}$, then:

$$\sum_{k \in [K]} \sum_{h=0}^{H-1} w_{\mathcal{F}_t}^2(s_h^k, a_h^k) \leq 1 + 4C^2 H \dim_E(\mathcal{F}, T^{-1/2}) + 4\beta_K \dim_E(\mathcal{F}, T^{-1/2}) (1 + \log T)$$

Proof. We first show the following lemma, which will be helpful in our proof.

Lemma 19 (Lemma 1 in [Osband and Van Roy, 2014]). *If $\{\beta_k\}_{k \in [K]}$ is a non-decreasing sequence, we have*

$$\sum_{k \in [K]} \sum_{h=0}^{H-1} \mathbf{1}_{w_{\mathcal{F}_k}(s_h^k, a_h^k) > \epsilon} \leq \left(\frac{4\beta_K}{\epsilon^2} + H \right) \dim_E(\mathcal{F}, \epsilon).$$

Proof. We first consider when $w_{\mathcal{F}_k}(s_h^k, a_h^k) > \epsilon$ and is ϵ -dependent on n disjoint sub-sequences of $\{(s_h^i, a_h^i)\}_{i \in [k-1]}$. By the definition of ϵ -dependent, we know $\|\bar{f} - \underline{f}\|_{2, E_k} > n\epsilon^2$. On the other hand, by triangle inequality, we know $\|\bar{f} - \underline{f}\|_{2, E_k} \leq 2\sqrt{\beta_k} \leq 2\sqrt{\beta_K}$, thus $n < \frac{4\beta_K}{\epsilon^2}$. Hence we know when $w_{\mathcal{F}_k}(s_h^k, a_h^k) > \epsilon$, then (s_h, a_h) is at most ϵ -dependent on $\frac{4\beta_K}{\epsilon^2}$ disjoint sub-sequences of $\{(s_h^i, a_h^i)\}_{i \in [k-1]}$.

We then show that, for any sequence $\{(s_i, a_i)\}_{i \in [N]}$, there is some element (s_j, a_j) that is ϵ -dependent on at least $\frac{n}{\dim_E(\mathcal{F}, \epsilon)} - H$ disjoint sub-sequences of $\{(s_i, a_i)\}_{i \in [j-1]}$. Let n satisfies that $n \dim_E(\mathcal{F}, \epsilon) + 1 \leq N \leq (n+1) \dim_E(\mathcal{F}, \epsilon)$, and we will construct n disjoint sub-sequences $\{B_i\}_{i \in [n]}$. We first let $B_i = \{(s_i, a_i)\}, \forall i \in [n]$. If (s_{k+1}, a_{k+1}) is ϵ -dependent on each $B_i, i \in [n]$, we have the desired results. Otherwise, we append (s_{k+1}, a_{k+1}) to the sub-sequence that it is ϵ -independent with. Repeat this process until some $j > n+1$ is ϵ -dependent on each sub-sequence or we have reached N . In the latter case we have $\sum_{i \in [n]} |B_i| \geq n \dim_E(\mathcal{F}, \epsilon)$ (here we can add at most $H-1$ data to avoid the case we need a new episode of data), and since each element of a sub-sequence is ϵ -independent with its predecessors, $|B_i| \leq \dim_E(\mathcal{F}, \epsilon), \forall i$ by the definition of eluder dimension. Thus $|B_i| = \dim_E(\mathcal{F}, \epsilon), \forall i$. And in this case, (s_N, a_N) must be ϵ -dependent on each sub-sequence by the definition of eluder dimension. Notice that, as our data is collected in an episodic pattern, there are at most $H-1$ sub-sequences that contains "imaginary" final episode data introduced to the construction. In this case, we know that there are at least $\frac{n}{\dim_E(\mathcal{F}, \epsilon)} - H$ disjoint sub-sequences that (s_N, a_N) is ϵ -dependent, which finishes our claim.

We finally consider the sub-sequence $B = \{(s_h^k, a_h^k)\}$ with $w_{\mathcal{F}_k}(s_h^k, a_h^k) > \epsilon$. We know that each element in B is ϵ -dependent on at most $\frac{4\beta_K}{\epsilon^2}$ disjoint sub-sequences of B , but at least ϵ -dependent on $\frac{|B|}{\dim_E(\mathcal{F}, \epsilon)} - H$ sub-sequences of B . Thus we know $|B| \leq \left(\frac{4\beta_K}{\epsilon^2} + H \right) \dim_E(\mathcal{F}, \epsilon)$, which concludes the proof. \square

For notation simplicity, we define $w_{t,h} := w_{\mathcal{F}_t}(s_h^t, a_h^t)$. We first reorder the sequence $\{w_{t,h}\}_{k \in [K], 0 \leq h \leq H-1} \rightarrow \{w_i\}_{i \in [KH]}$, such that $w_1 \geq \dots \geq w_{KH}$. Then we have

$$\sum_{k \in [K]} \sum_{h=0}^{H-1} w_{\mathcal{F}_t}^2(s_h^k, a_h^k) = \sum_{i \in [KH]} w_i^2 \leq \sum_{i \in [KH]} w_i^2 \mathbf{1}_{w_i < T^{-1/2}} + \sum_{i \in [KH]} w_i^2 \mathbf{1}_{w_i \geq T^{-1/2}} \leq 1 + \sum_{i \in [KH]} w_i^2 \mathbf{1}_{w_i \geq T^{-1/2}}.$$

As we order the sequence, $w_j \geq \epsilon$ means

$$\sum_{k \in [K]} \sum_{h=0}^{H-1} \mathbf{1}_{w_{\mathcal{F}_t}(s_h^k, a_h^k) > \epsilon} \geq j.$$

Hence we know

$$\epsilon \leq \sqrt{\frac{4\beta_K}{\frac{j}{\dim_E(\mathcal{F}, \epsilon)} - H}} = \sqrt{\frac{4\beta_K \dim_E(\mathcal{F}, \epsilon)}{j - H \dim_E(\mathcal{F}, \epsilon)}},$$

which means if $w_i \geq T^{-1/2}$, then $w_i < \min \left\{ 2C, \sqrt{\frac{4\beta_K \dim_E(\mathcal{F}, T^{-1/2})}{k - H \dim_E(\mathcal{F}, T^{-1/2})}} \right\}$. Hence,

$$\begin{aligned} \sum_{i \in [KH]} w_i^2 \mathbf{1}_{w_i \geq T^{-1/2}} &\leq 4C^2 H \dim_E(\mathcal{F}, T^{-1/2}) + \sum_{j=H \dim_E(\mathcal{F}, T^{-1/2})+1}^T \frac{4\beta_K \dim_E(\mathcal{F}, T^{-1/2})}{j - H \dim_E(\mathcal{F}, T^{-1/2})} \\ &\leq 4C^2 H \dim_E(\mathcal{F}, T^{-1/2}) + 4\beta_K \dim_E(\mathcal{F}, T^{-1/2}) (1 + \log T), \end{aligned}$$

which finishes the proof. \square

C.4 PROOF FOR THEOREM 5 AND THEOREM 12

Proof. Define $\mathcal{E}_k = \mathbb{P}_{f^*}(f^* \in \mathcal{F}_k)$. When constructing the confidence set, take $\alpha = T^{-1/2}$ and $\delta = 0.25$ in Lemma 11, which leads to

$$\beta_k^* := 8\sigma^2 \log(4\mathcal{N}(\mathcal{F}, T^{-1/2}, \|\cdot\|_2)) + HT^{-1/2}(12C + \sqrt{8d\sigma^2 \log(16k^2H)}).$$

With our confidence set construction, we know that $\sum_{k \in [K]} P(\bar{\mathcal{E}}_k) \leq 0.5$. Notice that

$$\begin{aligned} \text{Regret}(K) &= \sum_{k \in [K]} [V_0^*(s_0^k) - V_0^{\pi_k}(s_0^k)] \\ &\leq \mathbb{E} \left[\sum_{k \in [K]} \mathbb{E} [\mathbb{P}(\mathcal{E}_k) [V_0^*(s_0^k) - V_0^{\pi_k}(s_0^k)]] \right] + H \sum_{k \in [K]} \mathbb{P}(\bar{\mathcal{E}}_k) \\ &\leq \mathbb{E} \left[\sum_{k \in [K]} \mathbb{E} [\tilde{V}_{0,k}^{\pi_k}(s_0^k) - V_0^{\pi_k}(s_0^k)] \right] + 0.5H \\ &\leq H^{3/2} \sum_{k \in [K]} \sqrt{\mathbb{E} \left[\sum_{h=0}^{H-1} \min \left\{ \frac{2\|\tilde{f}_k(s_h^k, a_h^k) - f^*(s_h^k, a_h^k)\|_2^2}{\sigma^2}, 1 \right\} \right]} + 0.5H \\ &\leq \sqrt{H^2 T \mathbb{E} \left[\sum_{k \in [K]} \sum_{h=0}^{H-1} \min \left\{ \frac{2\|\tilde{f}_k(s_h^k, a_h^k) - \hat{f}^*(s_h^k, a_h^k)\|_2^2}{\sigma^2}, 1 \right\} \right]} + 0.5H \\ &\leq \sqrt{\frac{2H^2 T}{\sigma^2} (1 + 4C^2 H \dim_E(\mathcal{F}, T^{-1/2}) + 4\beta_K^* \dim_E(\mathcal{F}, T^{-1/2}) (1 + \log T))} + 0.5H, \end{aligned}$$

where the first equality is due to the fact that the total reward for each episode is bounded in $[0, H]$, the second inequality is due to the optimism and our confidence set construction, the third inequality is due to Lemma 14, the fourth inequality is due to Cauchy-Schwartz inequality and the final inequality is due to Lemma 18, which concludes the proof of Theorem 12. Following the idea of [Russo and Van Roy, 2013, 2014, Osband and Van Roy, 2014], we can translate the worst-case regret bound for UCB algorithm into the expected regret bound for TS algorithm, that conclude the proof of Theorem 5. \square

Remark It can be undesirable that our regret bound scale with σ^{-1} , which means our algorithm can perform pretty bad when the noise level is extremely low. It is also more or less counter-intuitive. We want to remark that, such phenomenon is only an artifact introduced by our proof strategy. The simulation lemma (Lemma 14) works well when $f(s, a) - \tilde{f}(s, a)$ is small. However, we need to tolerate some bad episodes to collect sufficient samples, that can eventually make the error small. Fortunately, the regret of such bad episode is at most H . Hence, we can use the following strategy to get rid of the dependency on σ^{-1} .

Definition 20 (Bad and Good Episodes). *Define episode k as a bad episode, if $\exists h \in \{0, 1, \dots, H-1\}$, such that $w_{k,h} := w_{\mathcal{F}_k}(s_h^k, a_h^k)$ is the largest $H \dim_E(\mathcal{F}, \sigma^2 T^{1/2})$ elements in the set $\{w_{k,h}\}_{k \in [K], 0 \leq h \leq H-1}$. Define episode k as a good episode, if it is not a bad episode.*

By the definition, we know there are at most $H \dim_E(\mathcal{F}, \sigma^2 T^{1/2})$ bad episodes. We then show the following lemma, that can be directly generalized from Lemma 18, by setting $\epsilon = \sigma^2 T^{-1/2}$ and remove the terms from bad episodes.

Lemma 21. *If $\{\beta_k^*\}_{k \in [K]}$ is a non-decreasing sequence, and $\|f\|_2 < C, \forall f \in \mathcal{F}$, then:*

$$\sum_{k \in [K], k \text{ is good}} \sum_{h=0}^{H-1} w_{\mathcal{F}_t}^2(s_h^k, a_h^k) \leq \sigma^2 + 4\beta_K \dim_E(\mathcal{F}, \sigma^2 T^{-1/2}) (1 + \log T)$$

Eventually, we can obtain the following regret bound, by setting the regret of bad episodes as H , and bounding the regret of good episodes with Lemma 21.

Theorem 22 (Improved Regret Bound). *Assume Assumption 2 to 5 holds. Take $\alpha = \sigma^2 T^{-1/2}$ and $\delta = 0.25$ in Lemma 11, which leads to*

$$\beta_k^* := 8\sigma^2 \log(4\mathcal{N}(\mathcal{F}, \sigma^2 T^{-1/2}, \|\cdot\|_2)) + H\sigma^2 T^{-1/2} (12C + \sqrt{8\delta\sigma^2 \log(16k^2 H)}).$$

We have that

$$\text{Regret}(K) \leq \sqrt{H^2 T \left(\frac{8\beta_K}{\sigma^2} + 1 \right) \dim_E(\mathcal{F}, \sigma^2 T^{-1/2}) (1 + \log T)} + 0.5H + H^2 \dim_E(\mathcal{F}, \sigma^2 T^{-1/2})$$

We would like to remark, that the definition of bad and good episodes is only used for the proof. We don't need to make any modification on the algorithm. Notice that, as $\beta_k^* \propto \sigma^2$, our upper bound in Theorem 22 can only scale with σ^{-1} through the logarithm covering number $\log(4\mathcal{N}(\mathcal{F}, \sigma^2 T^{-1/2}, \|\cdot\|_2))$ and eluder dimension $\dim_E(\mathcal{F}, \sigma^2 T^{-1/2})$. When \mathcal{F} is a linear function class, both term should scale with $\text{polylog}(\sigma)$, that matches the result from [Kakade et al., 2020].

D BOUNDS ON THE COMPLEXITY TERM UNDER LINEAR REALIZABILITY

We provide the upper bound on the covering number and the eluder dimension of \mathcal{F} when $\mathcal{F} := \{\theta^\top \varphi : \theta \in \mathbb{R}^{d_\varphi \times d}, \|\theta\|_2 \leq W\}$ where $\varphi : \mathcal{S} \times \mathcal{A} \rightarrow \mathbb{R}^{d_\varphi}$ is some known feature map. We first make the following standard assumption:

Assumption 6 (Bounded Feature).

$$\|\varphi(s, a)\|_2 \leq B, \forall (s, a) \in \mathcal{S} \times \mathcal{A}.$$

D.1 COVERING NUMBER

Theorem 23 (Covering Number Bound). *We have that*

$$\mathcal{N}(\mathcal{F}, \epsilon, \|\cdot\|_2) \leq \left(1 + \frac{2BW}{\epsilon}\right)^{d_\varphi}.$$

Proof. Notice that, by Cauchy-Schwartz inequality, we have that

$$\max_{(s,a) \in \mathcal{S} \times \mathcal{A}} \|\varepsilon_i^\top \varphi(s, a)\|_2 \leq B \|\varepsilon_i\|_2, \quad \forall \varepsilon_i \in \mathbb{R}^{d_\varphi}.$$

Thus, denote $\varepsilon = [\varepsilon_i]_{i \in [d]}$, we have that

$$\max_{(s,a) \in \mathcal{S} \times \mathcal{A}} \|\varepsilon^\top \varphi(s, a)\|_2^2 = \max_{(s,a) \in \mathcal{S} \times \mathcal{A}} \sum_{i \in [d]} \|\varepsilon_i^\top \varphi(s, a)\|_2^2 \leq B^2 \sum_{i \in [d]} \|\varepsilon_i\|_2^2 = B^2 \|\varepsilon\|_2^2.$$

Hence, to find an ϵ -cover for \mathcal{F} , we just need to find an ϵ/B -cover of $\{\theta : \theta \in \mathbb{R}^{d_\varphi \times d}, \|\theta\|_2 \leq W\}$. By standard argument on the covering number of Euclidean space (e.g. Lemma 5.7 in [Wainwright, 2019]), we can conclude the desired result. \square

D.2 ELUDER DIMENSION

Theorem 24 (Eluder Dimension Bound). *We have that*

$$\dim_E(\mathcal{F}, \epsilon) \leq \frac{3d_\varphi e}{e-1} \log \left(3 + \frac{12W^2 B^2}{\epsilon^2}\right) + 1.$$

Proof. Our proof follows the idea in [Russo and Van Roy, 2013]. Define

$$w_k := \sup \left\{ (\theta_1 - \theta_2)^\top \varphi(s, a) : \sqrt{\sum_{i \in [k-1]} ((\theta_1 - \theta_2)^\top \varphi_i(s_i, a_i))^2} \leq \epsilon', \theta_1, \theta_2 \in \mathbb{R}^{d_\varphi \times d}, \|\theta_1\| \leq W, \|\theta_2\| \leq W \right\}.$$

For notation simplicity, define $\varphi_k := \varphi(s_i, a_i)$, $\theta := \theta_1 - \theta_2$, and $\Phi_k := \sum_{i \in [k-1]} \varphi_i \varphi_i^\top$. Obviously, we have that $\|\theta\| \leq 2W$. Moreover, by straightforward calculation, we know

$$\sum_{i \in [k-1]} ((\theta_1 - \theta_2)^\top \varphi_i(s_i, a_i))^2 = \text{Trace}(\theta^\top \varphi_k \theta).$$

Define $V_k := \Phi_k + \frac{(\epsilon')^2}{4W^2} I$, we start from considering the problem

$$\max_{\theta} \text{Trace}(\theta^\top \varphi_k \varphi_k^\top \theta), \quad \text{subject to} \quad \text{Trace}(\theta^\top V_k \theta) \leq 2\epsilon^2.$$

The Lagrangian can be formed as

$$\mathcal{L}(\theta, \gamma) = -\text{Trace}(\theta^\top \varphi_k \varphi_k^\top \theta) + \lambda (\text{Trace}(\theta^\top V_k \theta) - 2\epsilon^2), \quad \lambda \geq 0.$$

The optimality condition of θ is

$$(\lambda V_k - \varphi_k \varphi_k^\top) \theta = 0.$$

As V_k is of full rank, $\lambda V_k - \varphi_k \varphi_k^\top$ has rank at least $d_\varphi - 1$ (as $\varphi_k \varphi_k^\top$ is of rank 1). So the equation

$$(\lambda V_k - \varphi_k \varphi_k^\top) \theta_i = 0, \quad \theta_i \in \mathbb{R}^{d_\varphi}$$

only has one non-zero solution. Substitute back, we know that (define $\|x\|_A := \sqrt{x^\top A x}$):

$$\sup\{\text{Trace}(\theta^\top \varphi_k \varphi_k^\top \theta) : \text{Trace}(\theta^\top V_k \theta) \leq \epsilon^2\} = \sqrt{2\epsilon'} \|\varphi_k\|_{V_k^{-1}}.$$

With the conclusion above, we have that

$$w_k \leq \sup\{\theta^\top \varphi_k : \text{Trace}(\theta^\top \Phi_k \theta) \leq \epsilon^2, \|\theta\| \leq 2W\} \leq \sup\{\theta^\top \varphi_k : \text{Trace}(\theta^\top V_k \theta) \leq 2\epsilon^2\} = \sqrt{2}\epsilon' \|\varphi_k\|_{V_k^{-1}}.$$

Hence, if $w_k \geq \epsilon'$, then $\varphi_k^\top V_k^{-1} \varphi_k \geq 0.5$. Moreover, with Matrix Determinant Lemma, if $w_i \geq \epsilon', \forall i < k$, we have

$$\det(V_k) = \det(V_{k-1})(1 + \varphi_k^\top V_{k-1}^{-1} \varphi_k) \geq \det(V_{k-1}) \left(\frac{3}{2}\right) \geq \dots \geq \det\left(\frac{(\epsilon')^2}{4W^2} I\right) \left(\frac{3}{2}\right)^{k-1} = \frac{(\epsilon')^{2d}}{4W^{2d}} \left(\frac{3}{2}\right)^{k-1}.$$

Meanwhile,

$$\det(V_k) \leq \left(\frac{\text{Trace}(V_k)}{d}\right)^d \leq \left(\frac{B^2(k-1)}{d} + \frac{(\epsilon')^2}{4W^2}\right)^d.$$

Hence, we know

$$\left(\frac{3}{2}\right)^{(k-1)/d} \leq \frac{4W^2 B^2}{(\epsilon')^2} \cdot \frac{k-1}{d} + 1.$$

Now we only need to find the largest k that can make this inequality hold. For notation simplicity, define $\alpha := \frac{4W^2 B^2}{(\epsilon')^2}$, $n = \frac{k-1}{d}$. As $\log(1+x) \geq \frac{x}{1+x}$ and $\log x \leq x/e$, we have

$$\frac{n}{3} \leq n \log 3/2 \leq \log(\alpha + 1) + \log n \leq \log(\alpha + 1) + \log 3 + \log(n/3) \leq \log(\alpha + 1) + \log 3 + \frac{n}{3e}.$$

Substitute back, we can obtain the desired result. □

E EXPERIMENTAL DETAILS

E.1 ALGORITHM SUMMARY

Our algorithm is easily built on SAC. The only difference we make is we decouple the critic network into a representation network $\phi(\cdot)$ and a linear layer $l(\cdot)$ on top of the representation. The representation network is governed by the model dynamics loss in SPEDE, and we train a linear layer to predict the Q -value as it lies in the linear space of the representation guaranteed by our analysis. We update the representation by a momentum factor and keep the policy update the same procedure as SAC.

E.2 FULL EXPERIMENTS

Table 2: Performance of SPEDE on various MuJoCo control suite tasks. Our method achieve strong performance even comparing to pure empirical baselines. To be specific, in hard tasks like Humanoid-ET and Ant-ET, SPEDE outperforms the baselines significantly. Results with * are directly adopted from MBBL [Wang et al., 2019]. We also provide the SoTA model-free RL method SAC as a reference.

	Swimmer	Ant-ET	Hopper-ET	Pendulum
ME-TRPO*	30.1±9.7	42.6±21.1	4.9±4.0	177.3±1.9
PETS-RS*	42.1±20.2	130.0±148.1	205.8±36.5	167.9±35.8
PETS-CEM*	22.1±25.2	81.6±145.8	129.3±36.0	167.4±53.0
DeepSF	25.5±13.5	768.1±44.1	548.9±253.3	168.6±5.1
SPEDE	42.6±4.2	806.2±60.2	732.2±263.9	169.5±0.6
SAC*	41.2±4.6	2012.7±571.3	1815.5±655.1	168.2±9.5
	Reacher	Cartpole	I-pendulum	Walker-ET
ME-TRPO*	-13.4±5.2	160.1±69.1	-126.2±86.6	-9.5±4.6
PETS-RS*	-40.1±6.9	195.0±28.0	-12.1±25.1	-0.8±3.2
PETS-CEM*	-12.3±5.2	199.5±3.0	-20.5±28.9	-2.5±6.8
DeepSF	-16.8±3.6	194.5±5.8	-0.2±0.3	165.6±127.9
SPEDE	-7.2±1.1	138.2±39.5	0.0±0.0	501.58±204.0
SAC*	-6.4±0.5	199.4±0.4	-0.2±0.1	2216.4±678.7
	MountainCar	Acrobot	SlimHumanoid-ET	Humanoid-ET
ME-TRPO*	-42.5±26.6	68.1±6.7	76.1±8.8	776.8±62.9
PETS-RS*	-78.5±2.1	-71.5±44.6	320.7±182.2	106.9±102.6
PETS-CEM*	-57.9±3.6	12.5±29.0	355.1±157.1	110.8±91.0
DeepSF	-17.0±23.4	-74.4±3.2	533.8±154.9	241.1±116.6
SPEDE	50.3±1.1	-69.0±3.3	986.4±154.7	886.9±95.2
SAC*	52.6±0.6	-52.9±2.0	843.6±313.1	1794.4±458.3

E.3 ABLATIONS

Table 3: Ablation Study of SPEDE on MuJoCo tasks. We see that a small momentum factor help stabilize the performance, especially in environments like Huamoid and Hopper-ET.

	Hopper-ET	Ant-ET	S-Humanoid-ET	Humanoid-ET
SPEDE-0.9	593.2±37.4	877.7±45.9	881.6±385.2	232.9±63.4
SPEDE-0.99	305.9±13.4	707.9±51.1	629.3±106.9	818.1±130.6
SPEDE-0.999	732.2±263.9	806.2±60.2	986.4±154.7	886.9±95.2

Momentum Update Our ablation experiments are trying to study an important design choice of the practical algorithm: the momentum used to update the critic function. We summarize the results in Table 3. We can see that using a small large momentum factor such as 0.999 shows better performance. This is intuitively understandable: large momentum factor slows down the update speed of the representation of the critic function and thus stabilize the training. Such phenomenon illustrates the importance of slowly update the representation.

Random Feature Dimension We also conduct the experiments on how does the random feature dimension affect the final performance of the algorithm. We plot the results in HalfCheetah environment in Fig. 2. We can see that when we increasing the random feature dimension, we see a performance gain on the final return. This suggests that using a larger number of feature dimension would help the performance.

MLP Network for Critic Network We also conduct an experiment to study whether adding a MLP network on top of our representation could work. We show such ablation in Tab. 4. From the results, we see that the performance of MLP network is in generally better than the Linear network.

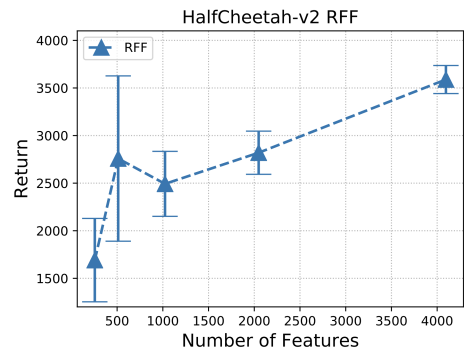


Figure 2: Increasing the number of random features can also lead to a performance gain.

Table 4: Comparison of SPEDE linear critic network and critic network. Results show that in general MLP network will further improve the performance.

	Reacher	MountainCar	Cartpole	Acrobot
SPEDE-Linear	-7.2±1.1	50.3±1.1	138.2±39.5	-69.0±3.3
SPEDE-MLP	-6.8±0.4	53.8±1.1	171.9±31.0	-15.6±1.9
SAC	-6.4±0.5	52.6±0.6	199.4±0.4	-52.9±2.0
	Pendulum	I-Pendulum	Walker-ET	S-Humanoid-ET
SPEDE-Linear	169.5±0.6	0.0±0.0	501.6±204.0	986.4±154.7
SPEDE-MLP	165.9±4.2	0.0±0.0	1005.7±458.4	2521.1±420.8
SAC	168.2±9.5	-0.2±0.1	2216.4±678.7	843.6±313.1

E.4 COMPARISON TO LC3

We provide a comparison of empirical results with LC3 [Kakade et al., 2020], which is also an algorithm with rigorous theoretical guarantees. Despite the major difference that we are learning the representation while LC3 assumes a given feature, the performance of SPEDE is much better than LC3 in tasks like Mountain Car and Hopper.

Table 5: Comparison of SPEDE with LC3 on MuJoCo tasks. LC3 only achieves good performance on relatively easy tasks like Reacher. However, their performance on Hopper and Mountain-Car is much worse than SPEDE.

	Reacher	MountainCar	Hopper
SPEDE	-7.2±1.1	50.3±1.1	732.2±263.9
LC3	-4.1±1.6	27.3±8.1	-1016.5±607.4

E.5 PERFORMANCE CURVES

We provide an additional performance curve including ME-TRPO in Figure 3 for a reference.

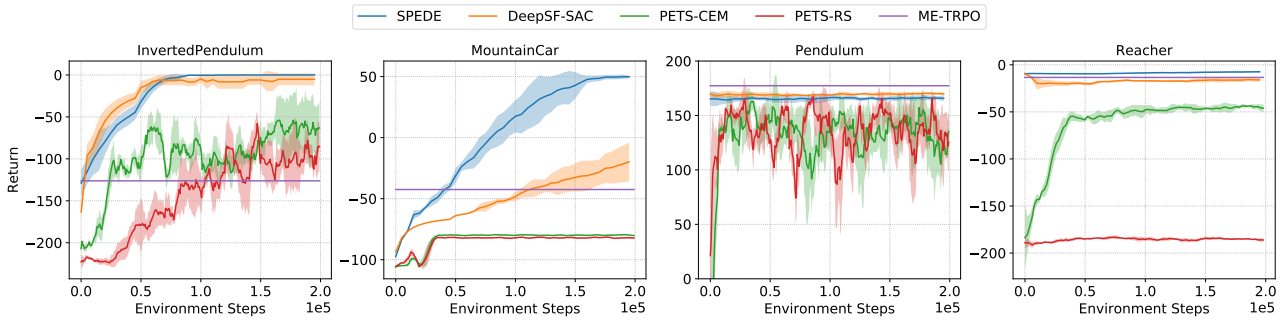


Figure 3: **Experiments on MuJoCo:** We show curves of the return versus the training steps for SPEDE and model-based RL baselines. We also include the final performance of ME-TRPO from [Wang et al., 2019] for reference.

E.6 HYPERPARAMETERS

We conclude the hyperparameter we use in our experiments in the following.

Table 6: Hyperparameters used for SPEDE in all the environments in MuJoCo.

	Hyperparameter Value
Actor lr	0.0003
Model lr	0.0001
Actor Network Size	(1024, 1024, 1024)
Fourier Feature Size	1024
Discount	0.99
Target Update Tau	0.005
Model Update Tau	0.001
Batch Size	256